Search for Hybrid Baryons with CLAS12 experimental setup

Baryons 2016

Lucilla Lanza, Ph. D. student

Supervisor: prof. Annalisa D'Angelo

University of Rome, Tor Vergata

INFN

19 May 2016

Outline

Physics motivation: Search of Hybrid Baryons contributions in the low Q^2 evolution of the cross section for $K^+\Lambda$ electro-production in CLAS12

- Endorsement of a LoI by the Program Advisory Committee, PAC43.
- PAC44 Proposal

- **CLAS12 and FT @ JLAB**: experimental setup description.

- **Simulation and fast mc reconstruction** of $K^+\Lambda$ electro-production events in CLAS12

- **Sensitivity to electrocouplings**: statistical significance, Legendre moments, hybrid baryon mass blind fitting analysis to study the sensitivity of our system to the presence of an hybrid contribution

Hybrid Baryons

Hybrid Baryons: baryons with explicit gluonic degrees of freedom

Augmenting the quarks q by gluons g leads to **additional states** in the spectrum relative to the expectations of the model accounting for constituent quarks only. Physically allowed (color singlets) states in the baryon spectrum may be constructed from |qqqg> «hybrid» basis states, in addition to the familiar |qqq> quark model states.

Hybrid Baryons in LQCD

QCD allows for the existence of Hybrid Baryons.

LQCD predicts several hybrid baryons states.

J. Dudek et al, Hybrid Baryons in QCD, Phys.Rev. D85 (2012) 054016

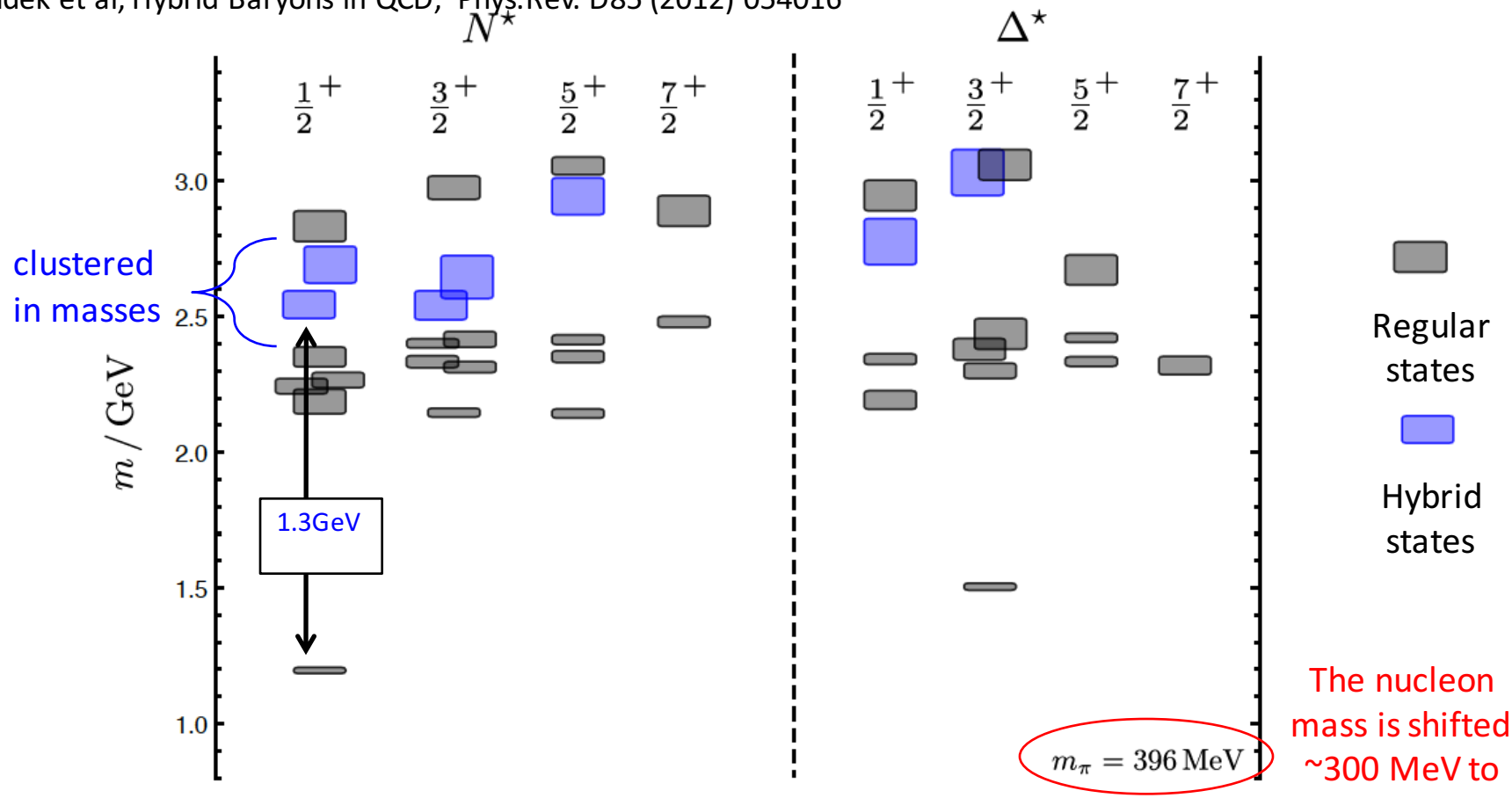

The nucleon mass is shifted ~300 MeV to higher masses

Differently from the case of hybrid mesons, hybrid baryons are predicted to have **same quantum numbers** of N* resonances

Separating Q^3G from Q^3 states: $A_{1/2,\,3/2}(Q^2)$ and $S_{1/2}(Q^2)$

Transverse helicity amplitude $A_{1/2}(Q^2)$, $A_{3/2}(Q^2)$ and longitudinal helicity amplitude $S_{1/2}(Q^2)$ allow to distinguish Q^3G from Q^3 states

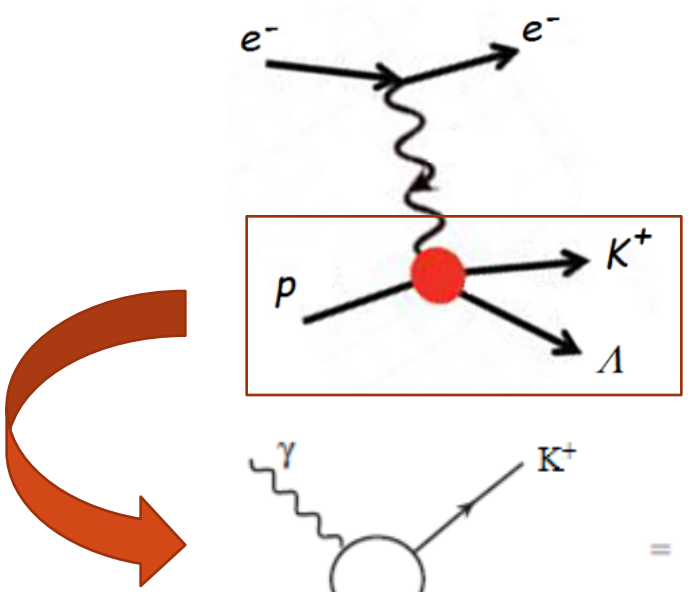

Electroexcitation via quasi-real photon exchange can be considered for practical purposes photo-production

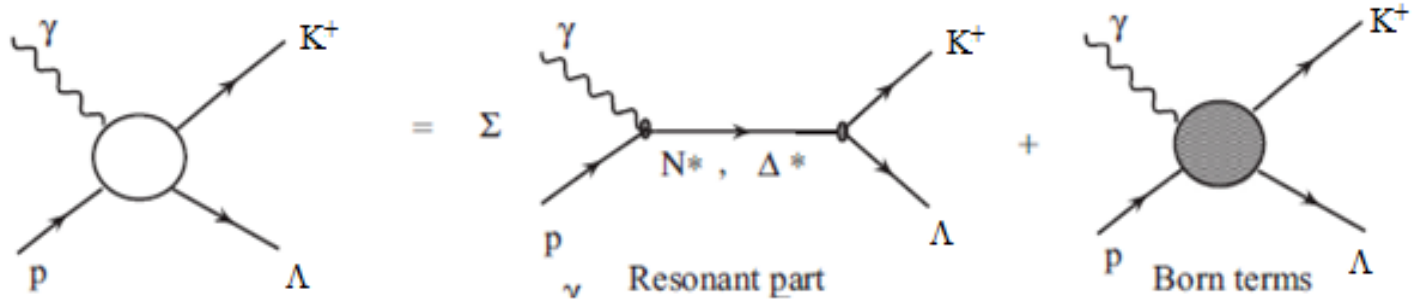

V. I. Mokeev, CLAS Collaboration, PHYSICAL REVIEW C 86, 035203 (2012)

Separating Q^3G from Q^3 states: $A_{1/2,\,3/2}(Q^2)$ and $S_{1/2}(Q^2)$

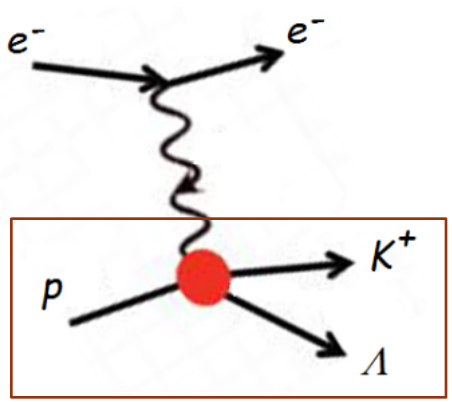

Resonant contribution in the helicity representation

Helicities of final state hadrons — Helicities of γ and p — N* helicity = $\lambda_\gamma - \lambda_p$

$$\langle \lambda_f | T_r | \lambda_\gamma \lambda_p \rangle = \sum_{N^*} \frac{\langle \lambda_f | T_{dec} | \lambda_R \rangle \langle \lambda_R | T_{em} | \lambda_\gamma \lambda_p \rangle}{M_r^2 - W^2 - i\Gamma_r(W) M_r}$$

where

Resonance mass — Invariant mass — Energy dependent total width

The ***N*** **hadronic decay amplitudes** can be expanded in **partial waves** of total momentum *J*

$$\langle \lambda_f | T_{dec} | \lambda_R \rangle = \langle \lambda_f | T_{dec}^{J_r} | \lambda_R \rangle d_{\mu\nu}^{J_r}(\cos\theta^*) e^{i\mu\phi^*}$$

where

$$\langle \lambda_f | T_{dec}^{J_r} | \lambda_R \rangle = \frac{2\sqrt{2\pi}\sqrt{2J_r+1}\,M_r\sqrt{\Gamma_{\lambda_f}}}{\sqrt{\langle p_i^r \rangle}} \sqrt{\frac{\langle p_i^r \rangle}{\langle p_i \rangle}}$$

The **resonance electroexcitation amplitudes** can be related to the $\gamma_v NN^*$ electrocouplings $\mathbf{A_{1/2}}$, $\mathbf{A_{3/2}}$, and $\mathbf{S_{1/2}}$ for nucleons

$$\langle \lambda_R | T_{em} | \lambda_\gamma \lambda_p \rangle = \frac{W}{M_r}\sqrt{\frac{8 M_N M_r q_{\gamma_r}}{4\pi\alpha}}\sqrt{\frac{q_{\gamma_r}}{q_\gamma}} A_{1/2,3/2}(Q^2) \quad \text{with} \quad |\lambda_\gamma - \lambda_p| = \frac{1}{2}, \frac{3}{2} \text{ for transverse photons,}$$

$$\langle \lambda_R | T_{em} | \lambda_\gamma \lambda_p \rangle = \frac{W}{M_r}\sqrt{\frac{16 M_N M_r q_{\gamma_r}}{4\pi\alpha}}\sqrt{\frac{q_{\gamma_r}}{q_\gamma}} S_{1/2}(Q^2) \text{ for longitudinal photons}$$

V. I. Mokeev, CLAS Collaboration, PHYSICAL REVIEW C 86, 035203 (2012)

Separating Q^3G from Q^3 states

Transverse helicity amplitude $A_{1/2}(Q^2)$ and longitudinal helicity amplitude $S_{1/2}(Q^2)$ allow to distinguish Q^3G from Q^3 states

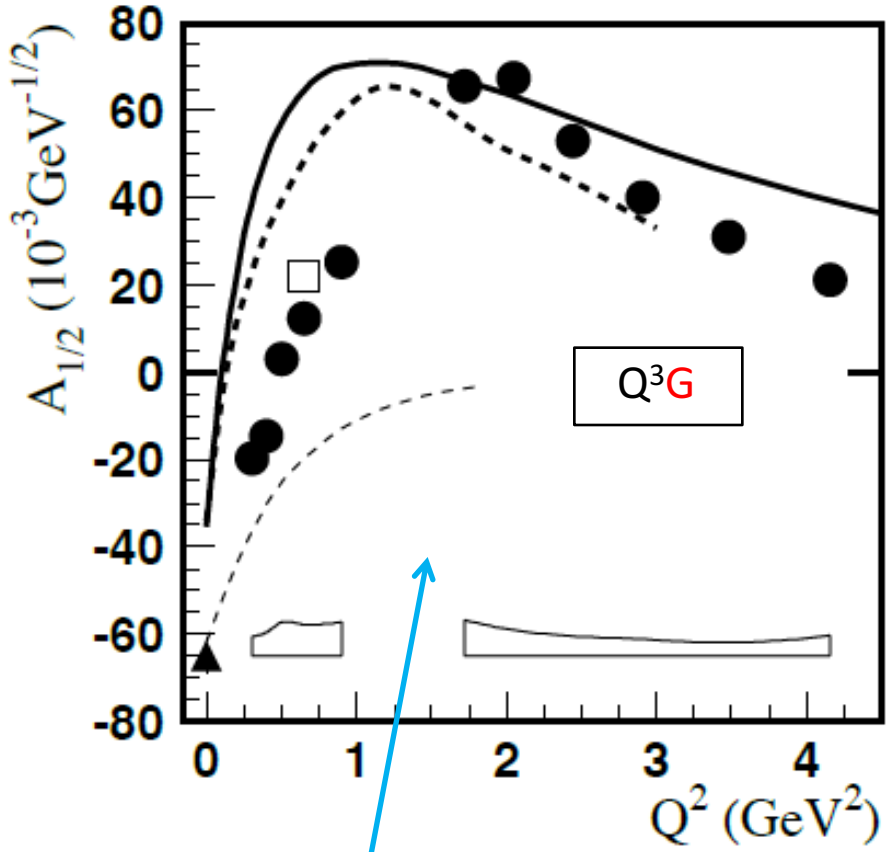

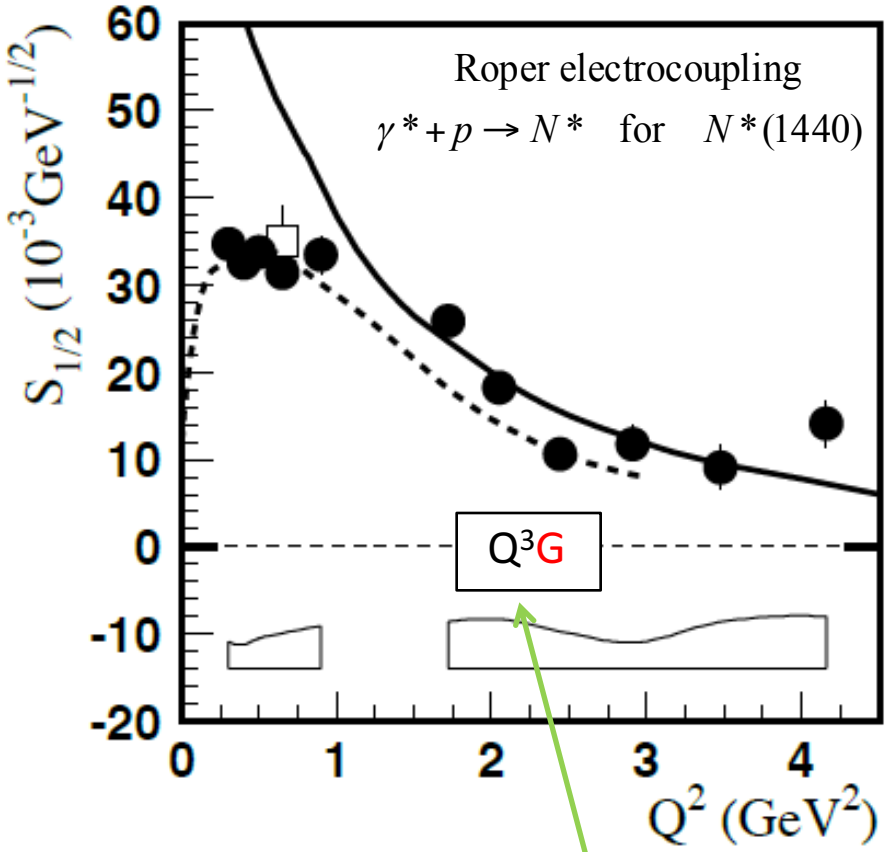

A drop of the transverse helicity amplitudes $A_{1/2}(Q^2)$ faster than for ordinary three quark states, because of extra glue-component in valence structure

A suppressed longitudinal amplitude $S_{1/2}(Q^2)$ in comparison with transverse electro-excitation amplitude

I. G. Aznauryan et al., CLAS Collaboration, PHYSICAL REVIEW C 80, 055203 (2009)

Signature

Based on available knowledge, the ***signature*** for hybrid baryons may consist of ***:***

- Extra resonances with $J^p=1/2^+$ and $J^p=3/2^+$, with masses from 1.8 GeV to 2.5 GeV and decays to $N\pi\pi$ or KY final states

- A drop of the transverse helicity amplitudes $A_{1/2}(Q^2)$ and $A_{3/2}(Q^2)$ faster than for ordinary three quark states, because of extra glue-component in valence structure

- A suppressed longitudinal amplitude $S_{1/2}(Q^2)$ in comparison with transverse electro-excitation amplitude

Experiment

Scattered electrons will be detected in Forward Tagger for angles from 2.5° to 4.5°. FT allows to probe the **crucial Q^2 range** where hybrid baryons may be identified due to their fast dropping $A_{1/2}(Q^2)$ amplitude and the suppression of the scalar $S_{1/2}(Q^2)$ amplitude.

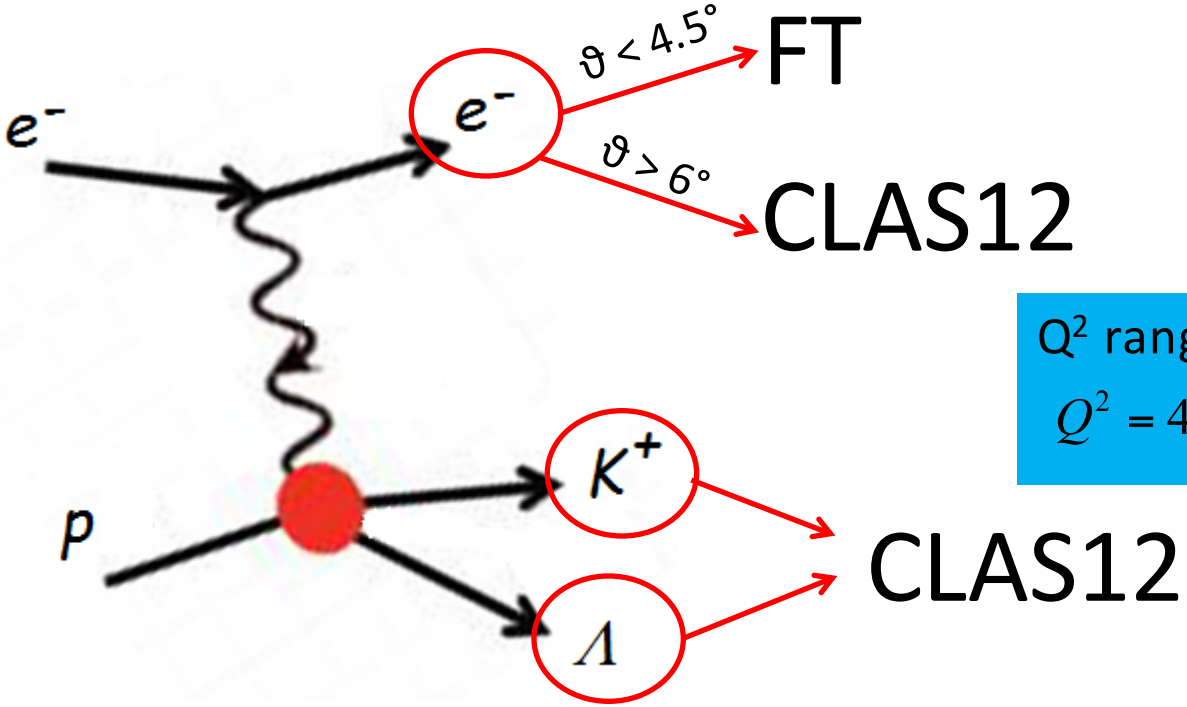

Q^2 range of interest: 0.05 - 2 GeV^2

$$Q^2 = 4E_{Beam}E_{e'}\sin^2\frac{\vartheta}{2} \quad \Rightarrow \quad \vartheta < 5°$$

Scattered electrons will be detected in the Forward Detector of CLAS12 for scattering angles greater than about 6°. Charged hadrons will be measured in the full range from 6° to 130°.

Experimental setup: CEBAF

Important parameters:

- Injector energy 45 MeV
- Temporal separation of the bunches 0,7 ns
- Halls A, B, C receive a 11 GeV electron beam, Hall D a 12 GeV electron with a 2 ns time interval
- The beam can be considered almost continuum because of the high work frequency
- Maximal intensity of the electron beam 200 µA
- P_b (long. polarization) up to 90%

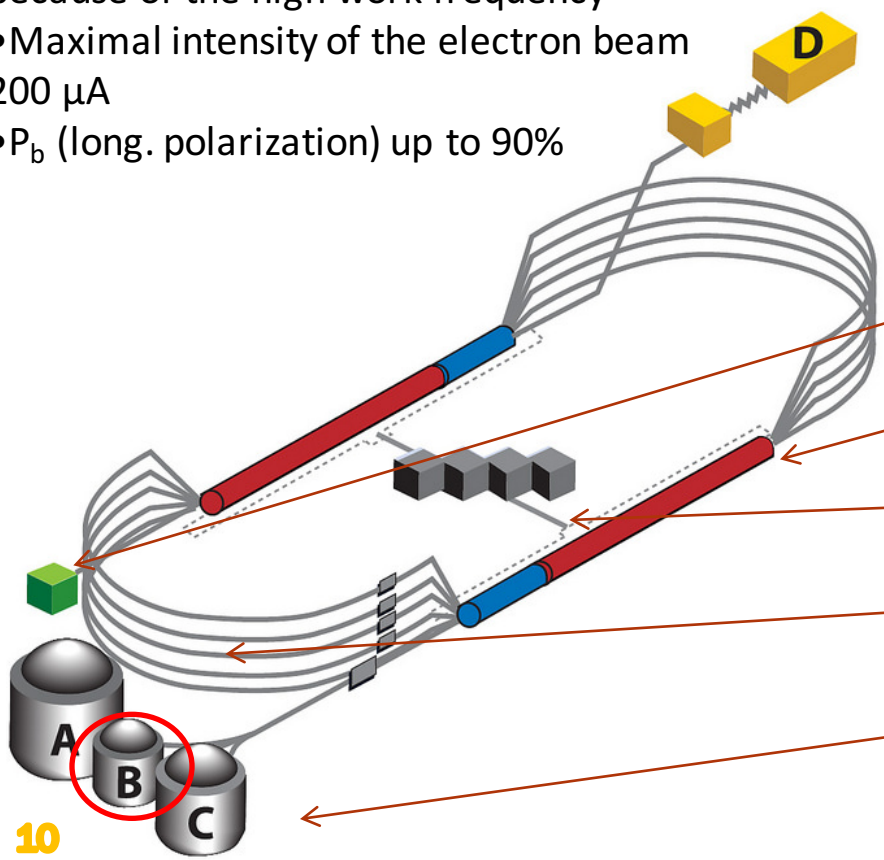

Components:

- **Iniector**: At nearly the speed of light, the electron beam circulates the 7/8 mile track in 24 millionths of a second
- **LINAC**: superconducting technology is used to drive electrons to higher and higher energies.
- **Refrigeration plant**: provides liquid helium for ultra-low-temperature, superconducting operation
- **Magnets**: in the arcs steer the electron beam from one straight section of the tunnel to the next for up to five orbits
- **Experimental Halls**: where the electron beam is delivered for simultaneous research by three teams of physicists

Experimental setup: CLAS12

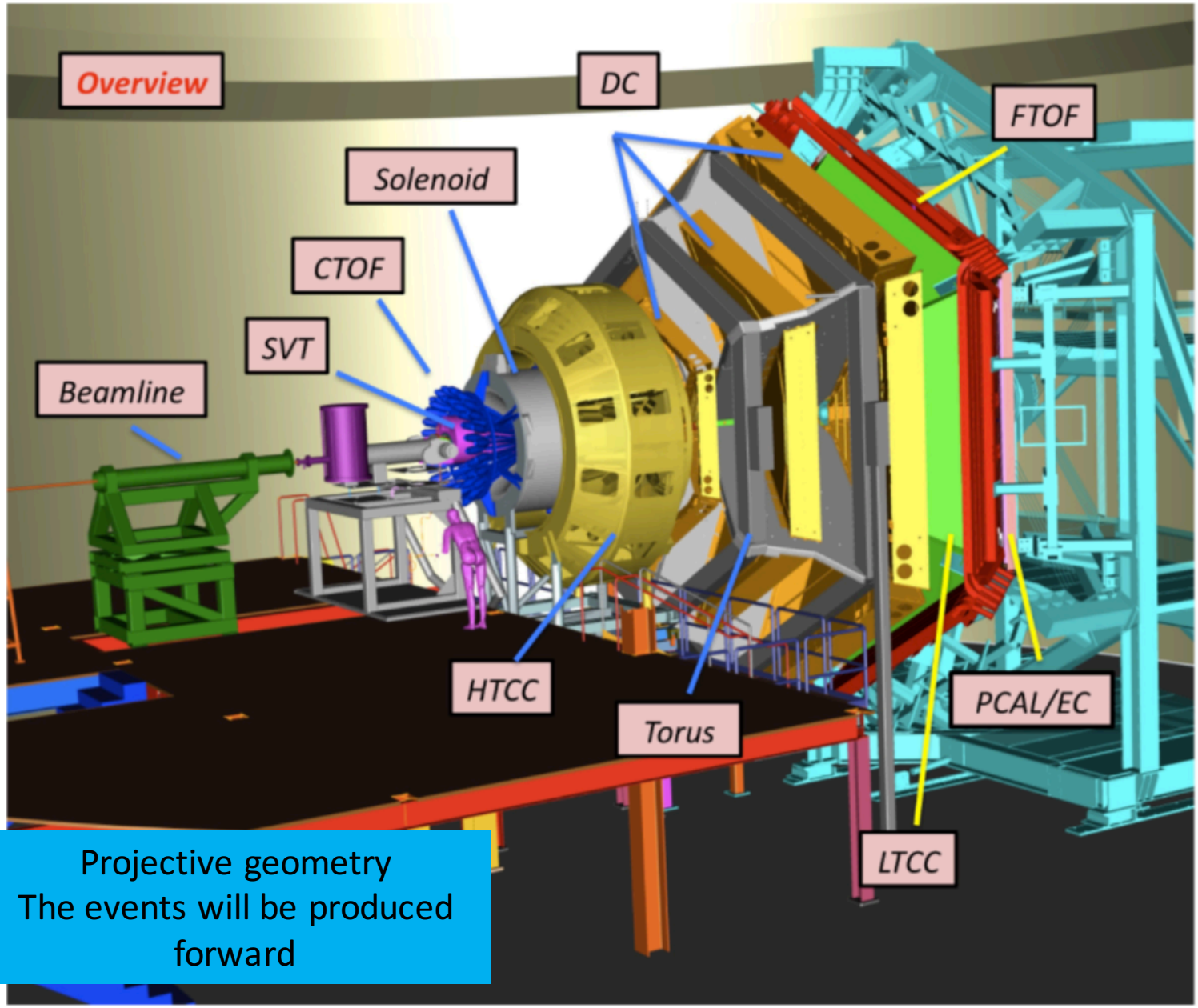

Projective geometry
The events will be produced forward

Experimental Setup: Forward Tagger (FT)

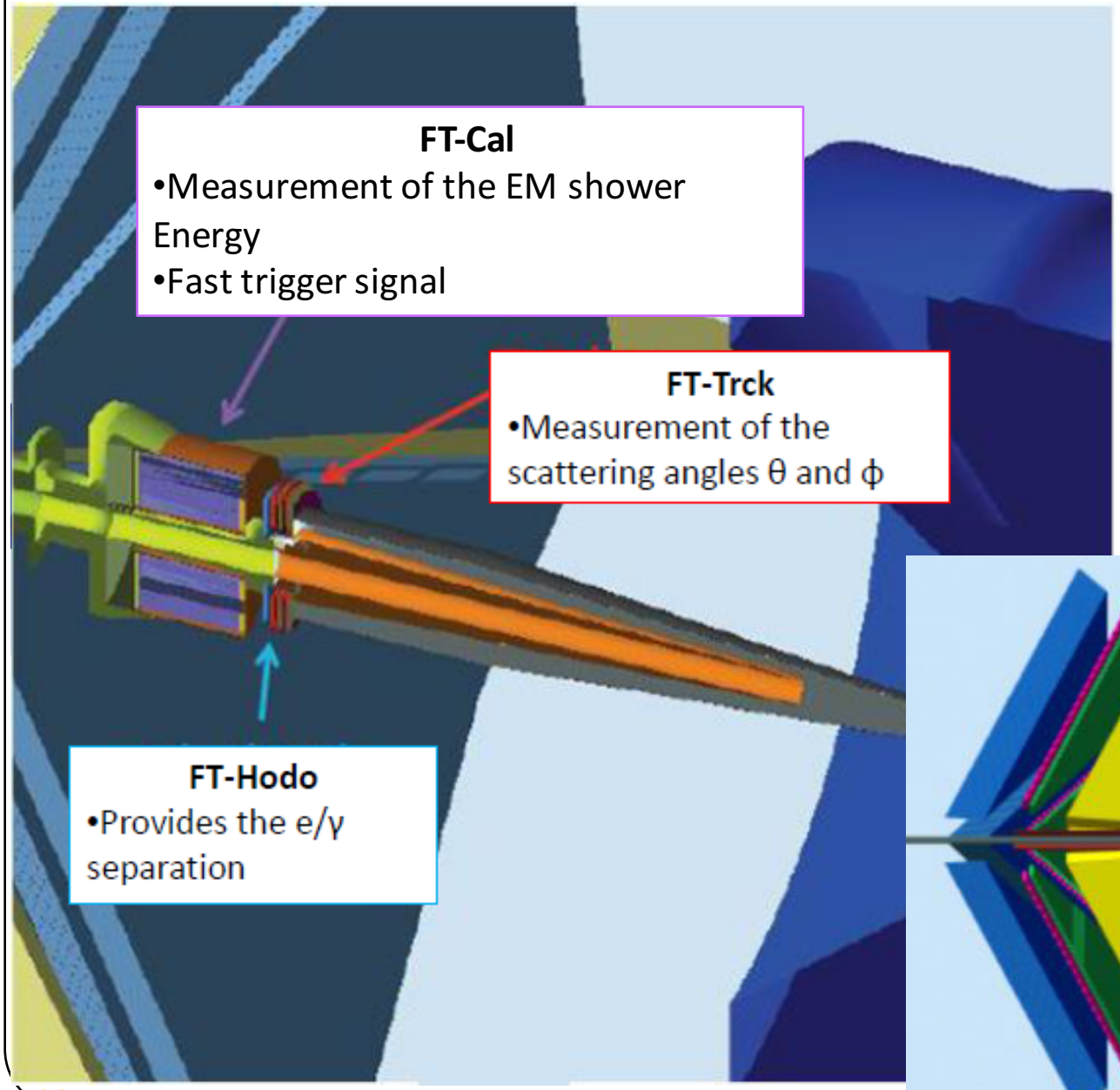

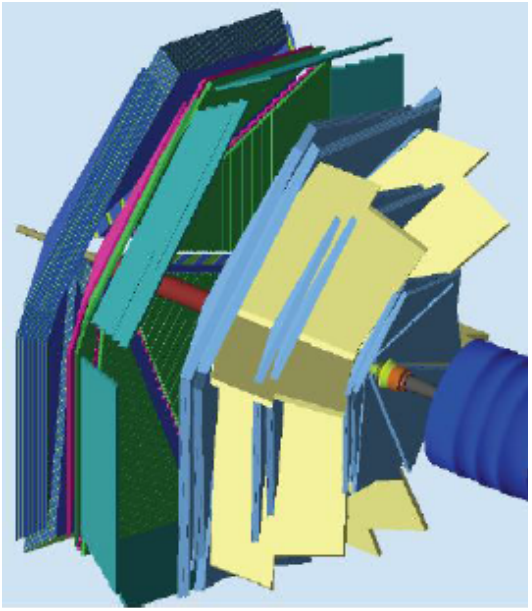

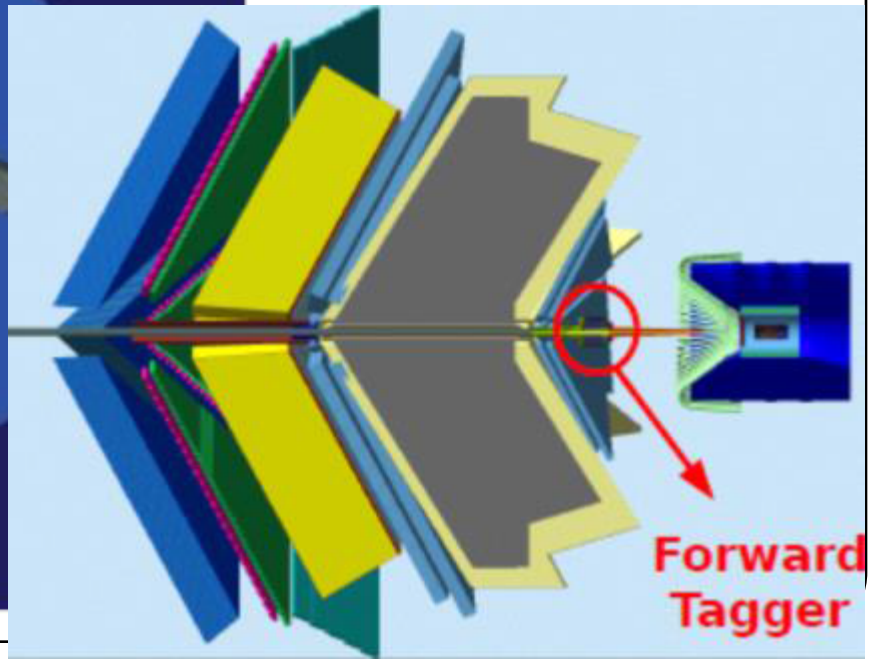

Hodoscope (FT-Hodo), Tracker (FT-Trck), and Calorimeter (FT-Cal)

Micromegas detectors exploit the gas ionization process with charged particles to Reconstruct the electron point of impact and path

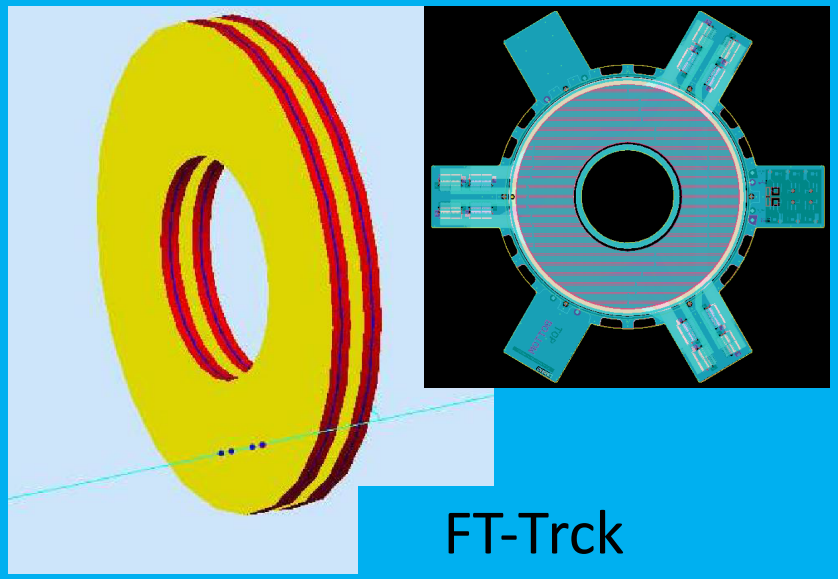

FT-Trck

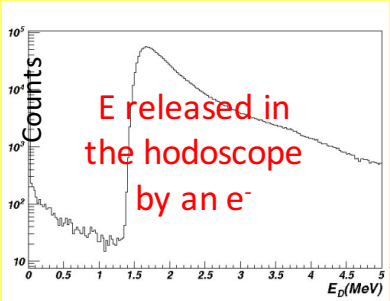

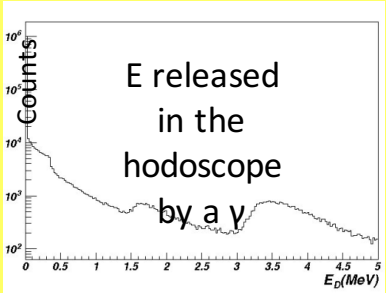

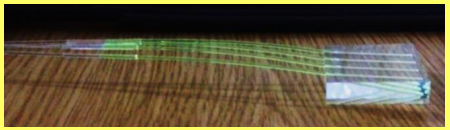

232 scintillator tiles, 752 fibers in total

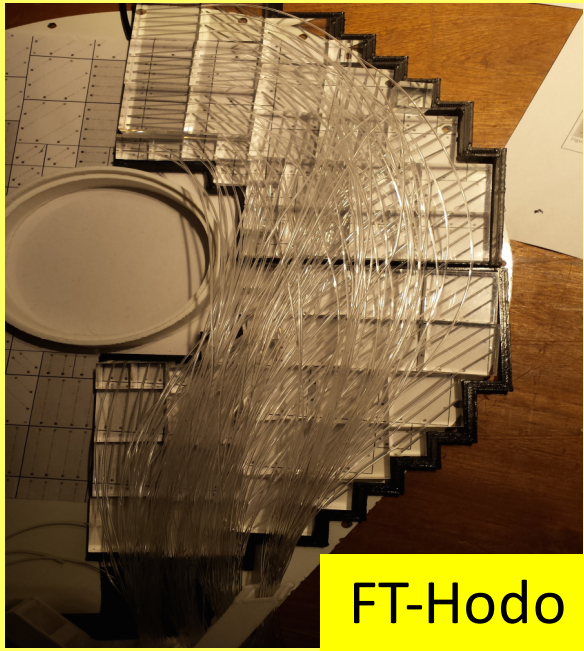

FT-Hodo

Requirements:
- High radiation hardness
- High light yield
- Small radiation length and Moliere radius
- Fast recovery time
- Good energy and time resolution

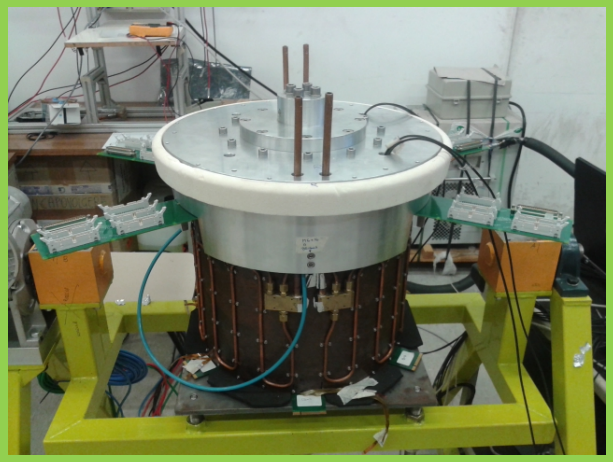

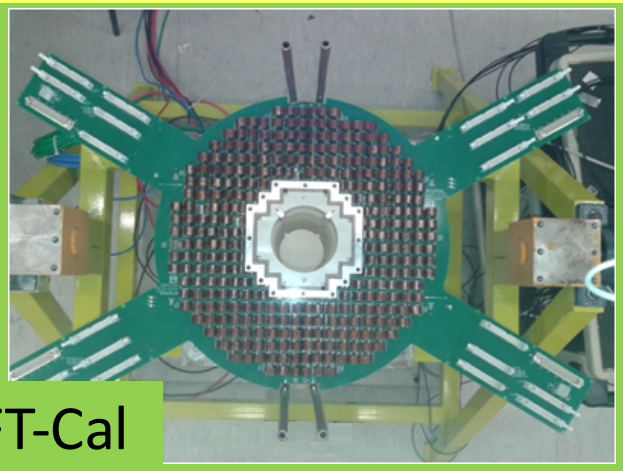

FT-Cal

Simulation and fast mc reconstruction of $K^+\Lambda$ electro-production events in CLAS12 using the Ghent RPR-2011 model

- Develop realistic event generator
- Simulation of *quasi-data* events including simplified experimental effects with FASTMC for channel

$$e + p \rightarrow e' + K^+ + \Lambda$$

- Selection of trigger conditions
- Production of events with different run conditions to extract the better configuration.

Available data on “Strange Calc” web site

http://rprmodel.ugent.be/calc/

StrangeCalc

Reaction type: Electroproduction

Reaction: $p(e,e'K^+)\Lambda$ $p(e,e'\pi^+)n$ $p(e,e'K^+)\Sigma^0$ $n(e,e'\pi^-)p$ $p(e,e'K^0)\Sigma^+$

Non-interference cross sections: $d\sigma_U$ $d\sigma_L$ $d\sigma_T$

Interference cross sections: $d\sigma_{LT}$ $d\sigma_{TT}$ $d\sigma_{LT'}$ $d\sigma_{TT'}$

Induced recoil polarization: $P^0_{y''}$ P^0_n

Transferred recoil polarization: $P'_{x''}$ $P'_{z''}$ P'_l P'_t

Clear

$x''y''z''$-frame: The z''-axis is along the virtual photon's three-momentum, the $x''z''$-plane is the electron plane, and the x''-axis' direction is such that the final electron's x''-component is positive.

ntl-frame: The l-axis is along the final baryon's three-momentum, the tl-plane is the hadron plane, and the t-axis' direction is such that the virtual photon's t-component is positive.

Energy variable: W s $E_{\gamma,\mathrm{c.m.}}$ $E_{\gamma,\mathrm{lab}}$

Fixed Range List

GeV

For the options 'Fixed' and 'Range', unphysical entries will be corrected if the variable's minimum/maximum value is not fixed. E.g.: $W = 0$ GeV will be corrected to $W = W_0$, with W_0 being the threshold energy, and $-t = 0$ GeV^2 will be corrected to $-t = -t_0$, with $-t_0$ being the minimum value of $-t$.

Angular variable: $\cos\theta_{\mathrm{c.m.}}$ $-t$ $-u$

Fixed Range List

Photon virtuality (Q^2): Fixed Range List

GeV^2

Model: RPR-2011 RPR-2007 VR

No resonance contributions

RPR-2011 model: Phys. Rev. C **86**, 015212 (2012)
RPR-2007 model: Phys. Rev. C **73**, 045207 (2006) and Phys. Rev. C **75**, 045204 (2007)
VR model: Phys. Rev. C **89**, 025203 (2014) and Phys. Rev. C **89**, 065202 (2014)

Calculate

StrangeCalc data have been used for the Event Generator.
From the collaboration with the Ghent group (Jan Rickebusch and Jannes Nys) we also obtained the RPR amplitudes.

Trigger and run conditions

Selection of trigger conditions for fastmc event generator

Selection of better run conditions for the experiment considering:

- E_{beam}= 6.6 GeV, 8.8 GeV, 11 GeV
- Torus current = ±1500 A, ±2950 A, ±3370 A

Magnetic field: inbending or outbending?

Q^2 vs W

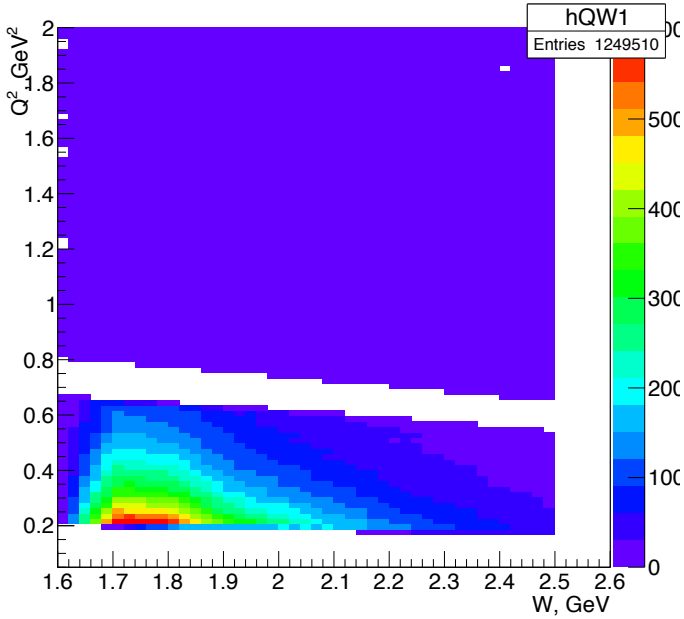

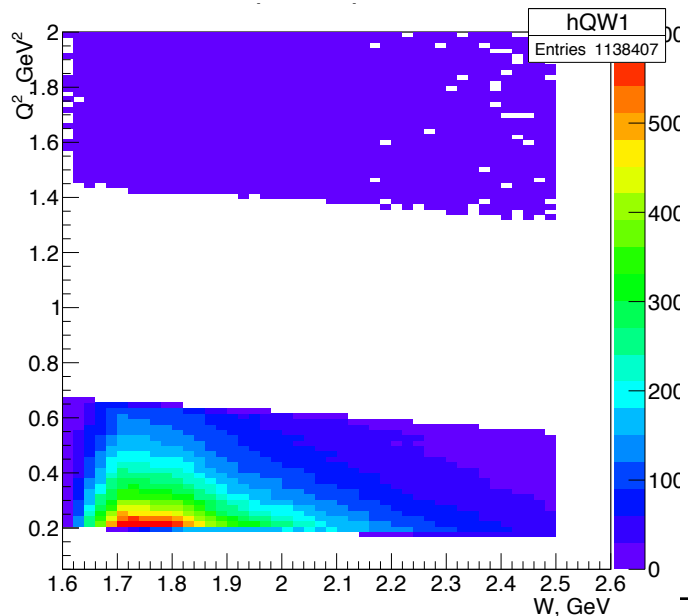

Efficiency curve

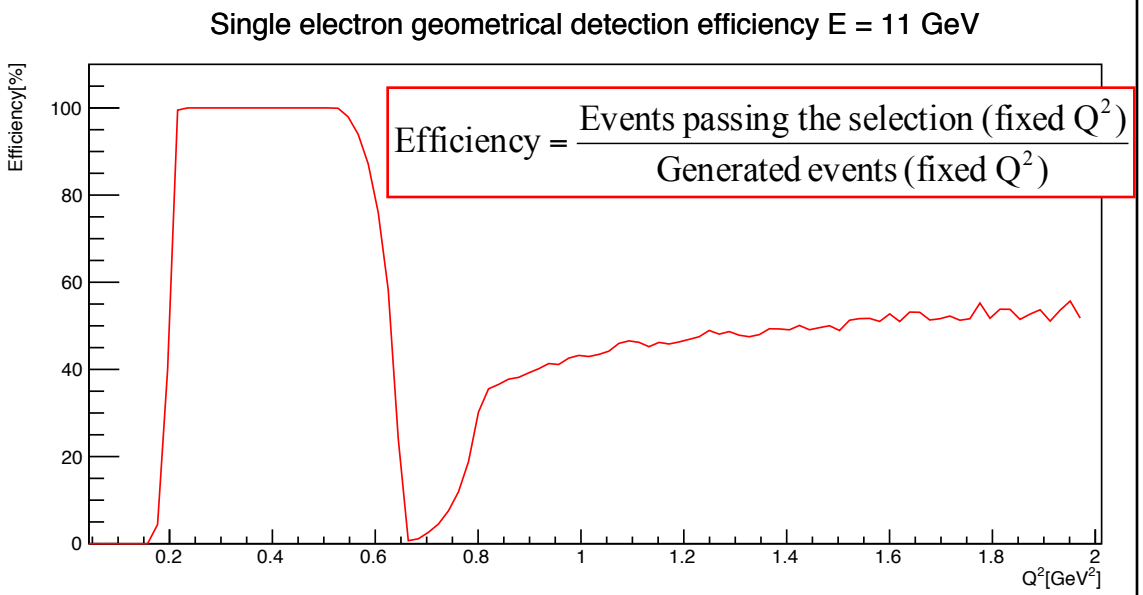

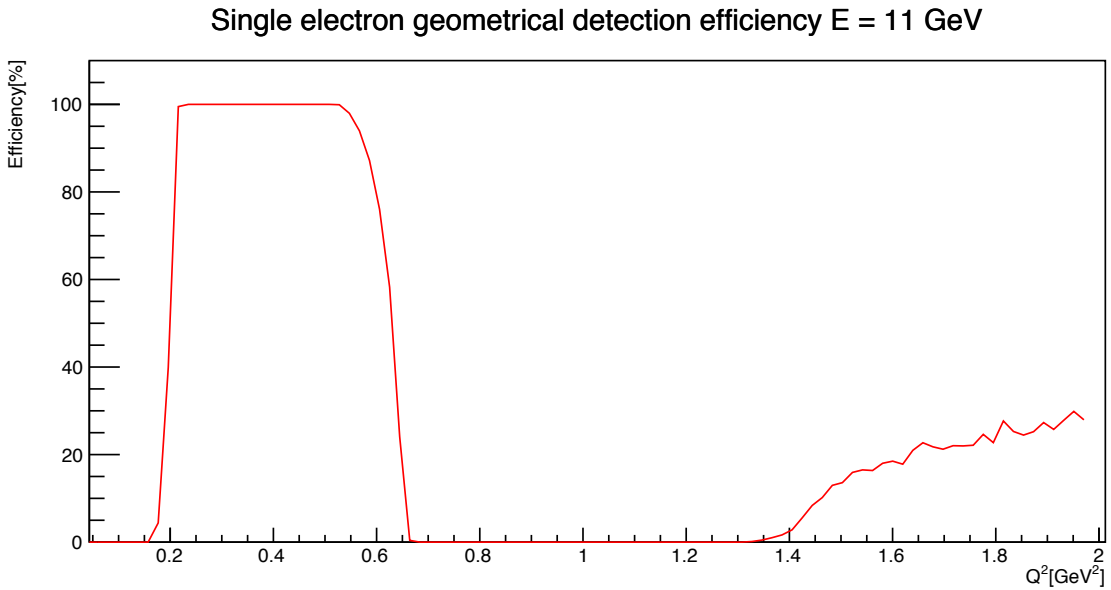

Strength of Torus current

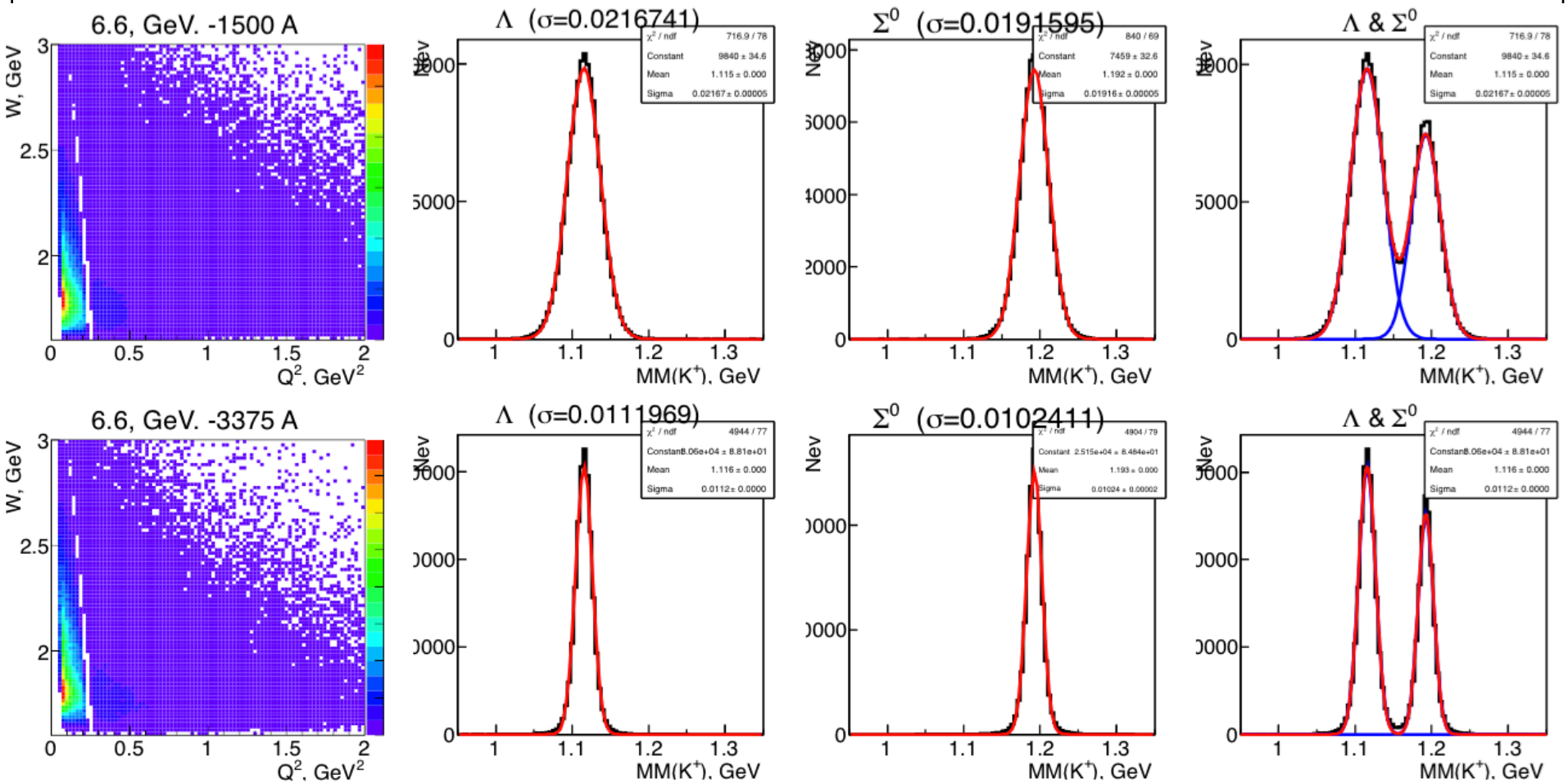

e'K⁺ missing mass to reconstruct Λ

e'K⁺ missing mass to reconstruct Σ^0

$K^+\Lambda$ and $K^+\Sigma^0$ overlap histograms

↓

Advantage of high CLAS12 torus currents

Covering the whole Q^2 range

Q^2 vs W

Efficiency curve

E = 6.6 GeV
TorCur= -3375 A

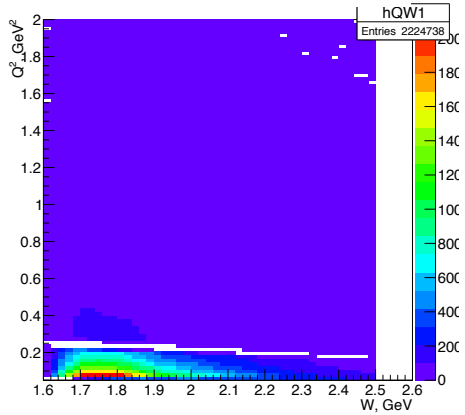

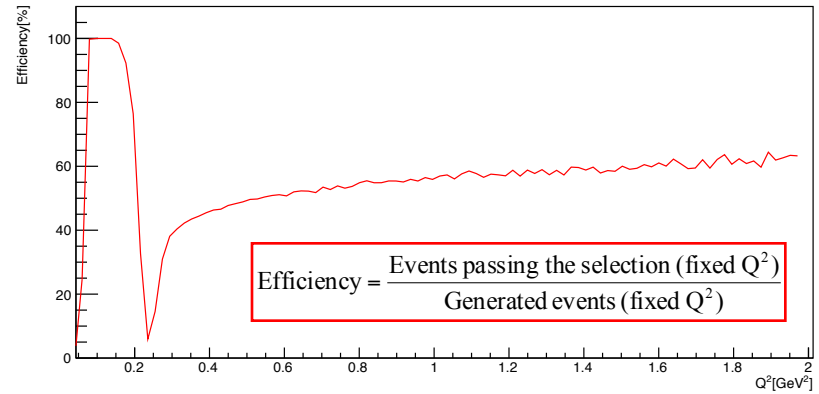

E = 8.8 GeV
TorCur= -3375 A

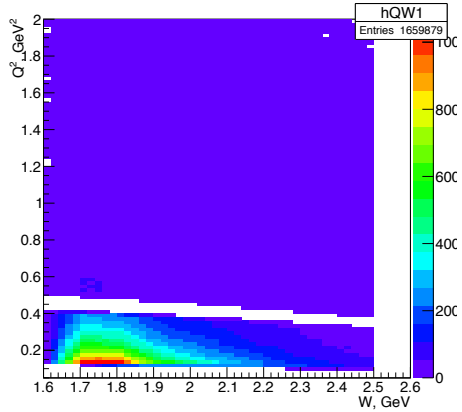

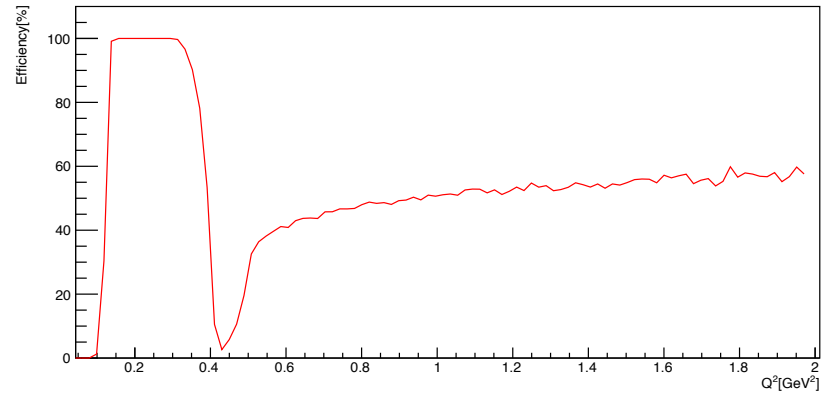

E = 11 GeV
TorCur= -3375 A

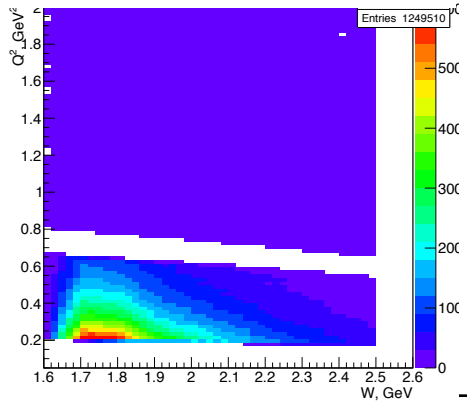

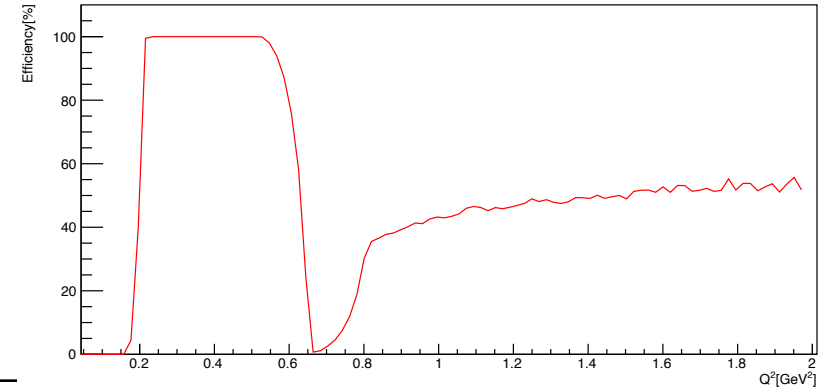

Covering the whole Q^2 range

Q^2 vs W

Efficiency curve

E = 6.6 GeV
TorCur= -3375 A

E = 8.8 GeV
TorCur= -3375 A

E = 11 GeV
TorCur= -3375 A

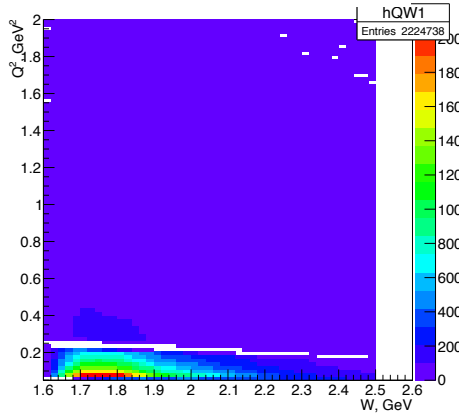

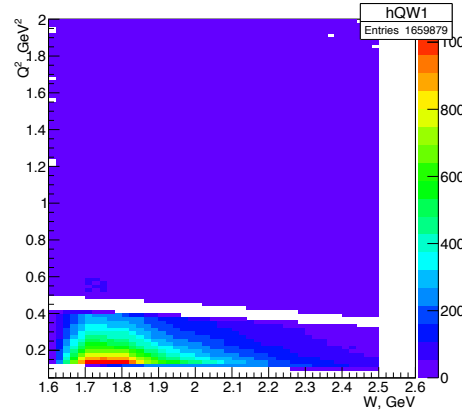

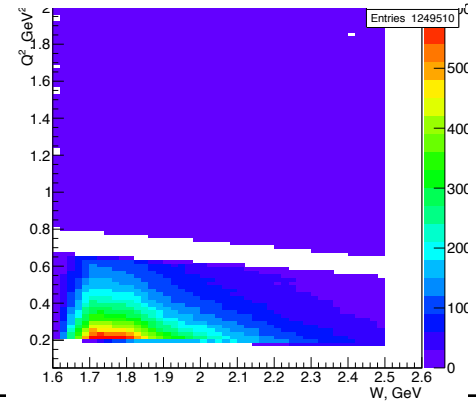

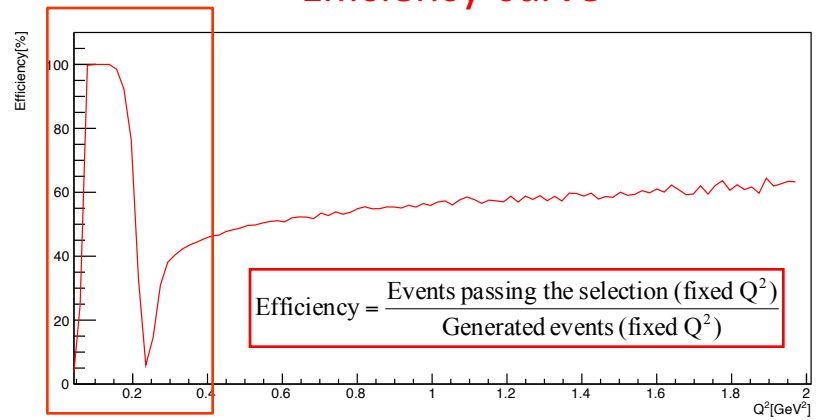

$$\text{Efficiency} = \frac{\text{Events passing the selection (fixed } Q^2)}{\text{Generated events (fixed } Q^2)}$$

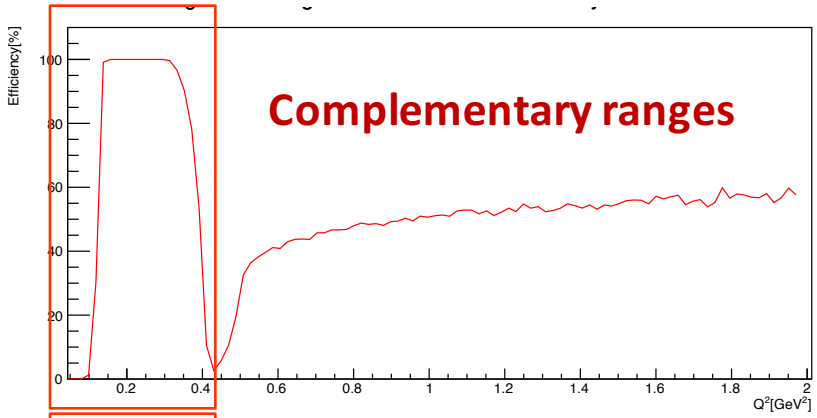

Complementary ranges

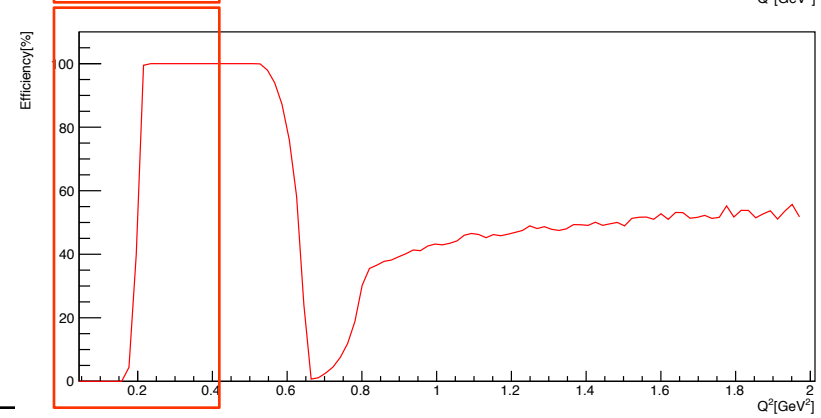

Results for run conditions: E_{beam}=6.6 GeV TorCur=-3375 A

ϕ vs ϑ for pion

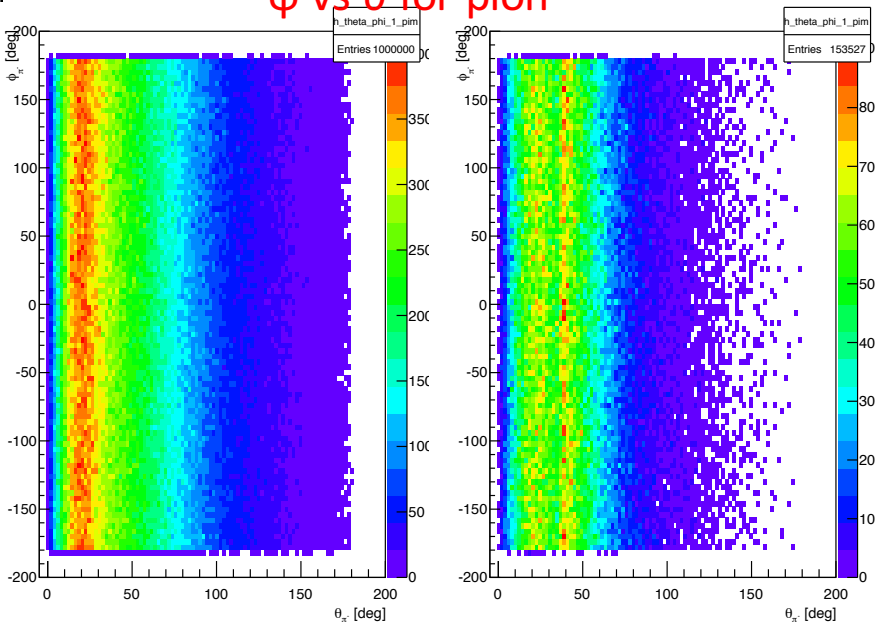

ϕ vs ϑ for kaon

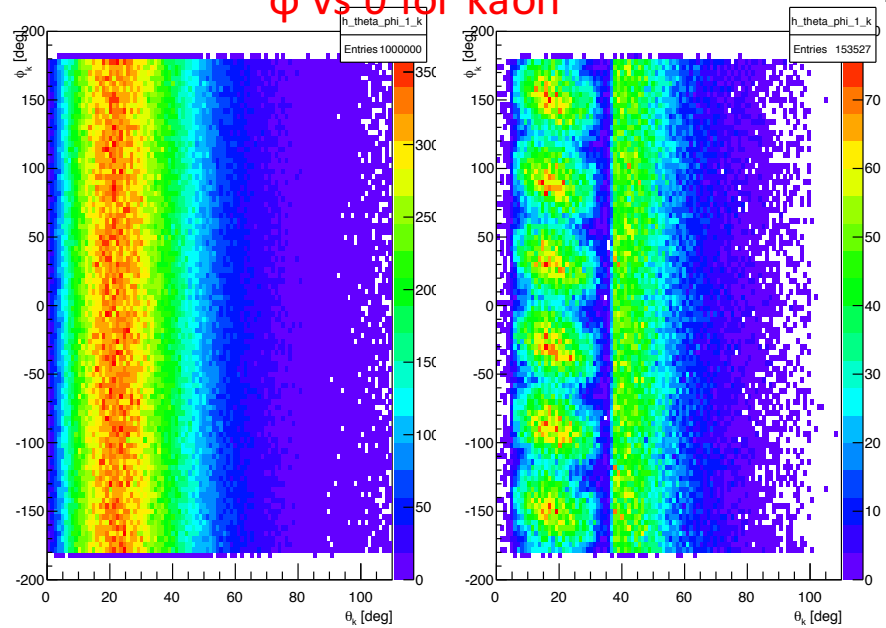

ϕ vs ϑ for proton

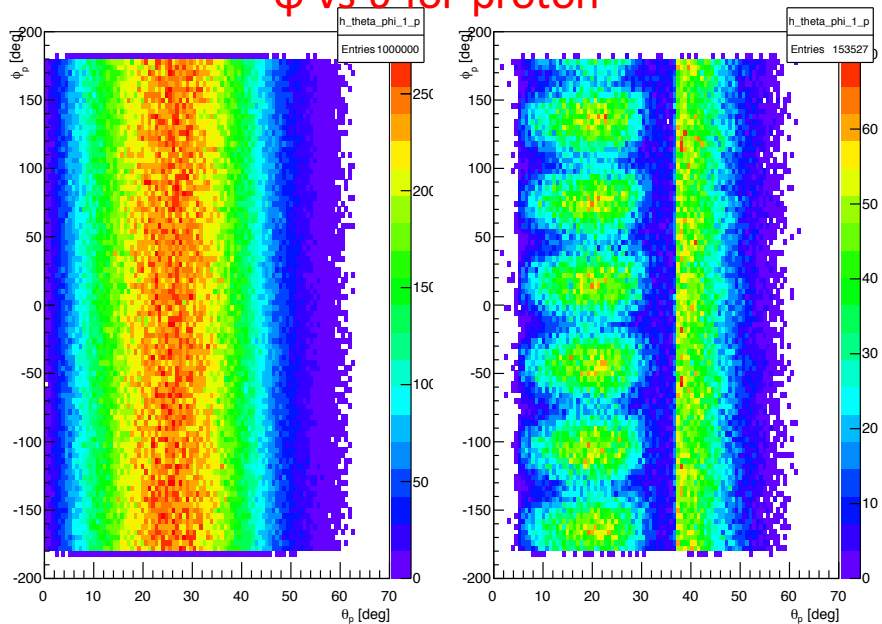

ϕ vs ϑ for electron

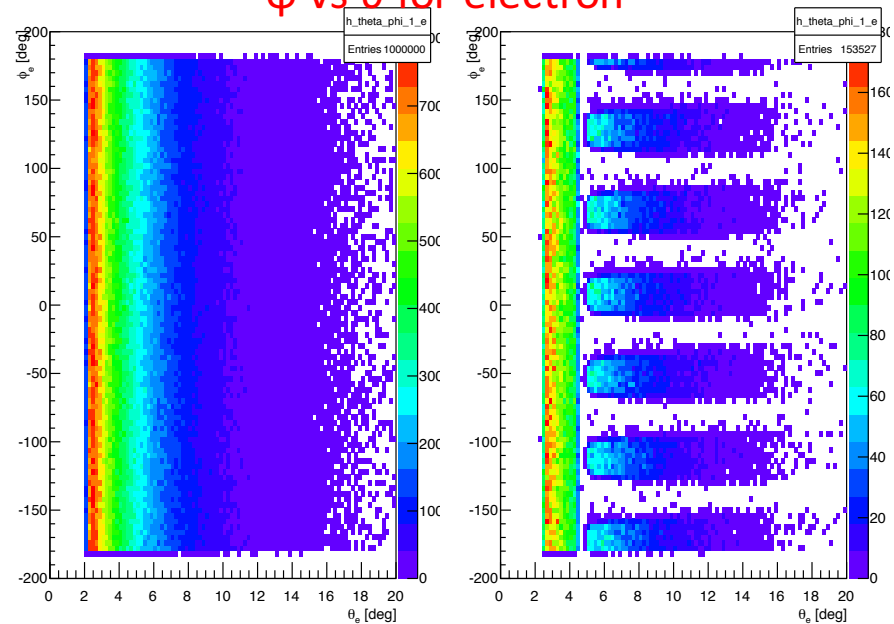

Simulation of RPR-2011 model + hybrid contribution

- Breit-Wigner ansatz for the hybrid amplitude:

$$M_{\lambda_\gamma}^{\lambda_p \lambda_Y} = \langle \lambda_f | T_r | \lambda_\gamma \lambda_p \rangle = \frac{\langle \lambda_f | T_{dec} | \lambda_R \rangle \langle \lambda_R | T_{em} | \lambda_\gamma \lambda_p \rangle}{M_r^2 - W^2 - i\Gamma_r M_r}$$

λ, λ_N, λ_Y = elicities of photon, nucleon and yperon

Dependence on the electrocouplings

$$\langle \lambda_R | T_{em} | \lambda_\gamma \lambda_p \rangle = \frac{W}{M_r} \sqrt{\frac{8 M_N M_r q_{\gamma_r}}{4\pi\alpha}} \sqrt{\frac{q_{\gamma_r}}{q_\gamma}} A_{1/2,3/2}(Q^2) \quad \text{with} \quad |\lambda_\gamma - \lambda_p| = \frac{1}{2}, \frac{3}{2} \text{ for transverse photons,}$$

$$\langle \lambda_R | T_{em} | \lambda_\gamma \lambda_p \rangle = \frac{W}{M_r} \sqrt{\frac{16 M_N M_r q_{\gamma_r}}{4\pi\alpha}} \sqrt{\frac{q_{\gamma_r}}{q_\gamma}} S_{1/2}(Q^2) \text{ for longitudinal photons}$$

- Add the hybrid contribution to the RPR-2011 at amplitude level:

$$\mathcal{M}_\lambda^{\lambda_N \lambda_Y} = M_\lambda^{\lambda_N \lambda_Y} + \mathscr{M}_\lambda^{\lambda_N \lambda_Y} \qquad \mathcal{H}_{\lambda\lambda'} = \sum_{\lambda_N, \lambda_Y} \mathcal{M}_\lambda^{\lambda_N \lambda_Y} \left(\mathcal{M}_{\lambda'}^{\lambda_N \lambda_Y} \right)^\dagger$$

Study of sensitivity

•Add the hybrid contribution at **amplitude level** and study the sensitivity of our system to the presence of a hybrid resonance:

$$\mathcal{M}_{\lambda}^{\lambda_N \lambda_Y} = M_{\lambda}^{\lambda_N \lambda_Y} + \mathscr{M}_{\lambda}^{\lambda_N \lambda_Y} \qquad \mathcal{H}_{\lambda\lambda'} = \sum_{\lambda_N, \lambda_Y} \mathcal{M}_{\lambda}^{\lambda_N \lambda_Y} \left(\mathcal{M}_{\lambda'}^{\lambda_N \lambda_Y}\right)^{\dagger}$$

λ, λ_N, λ_Y = elicities of photon, nucleon and yperon

•Using the relationships:

$$\frac{d\sigma_T}{d\Omega_K^*} = \chi \frac{1}{(4\pi)^2} (\mathcal{H}_{1,1} + \mathcal{H}_{-1,-1}) \qquad \frac{d\sigma_{TT}}{d\Omega_K^*} = -\chi \frac{1}{(4\pi)^2} (\mathcal{H}_{1,-1} + \mathcal{H}_{-1,1})$$

$$\frac{d\sigma_L}{d\Omega_K^*} = 2\chi \frac{1}{(4\pi)^2} \mathcal{H}_{0,0} \qquad \frac{d\sigma_{LT}}{d\Omega_K^*} = -\chi \frac{1}{(4\pi)^2} (\mathcal{H}_{0,1} + \mathcal{H}_{1,0} - \mathcal{H}_{-1,0} - \mathcal{H}_{0,-1})$$

$$\frac{d^5\sigma}{d\epsilon_2^{lab} d\Omega_2^{lab} d\Omega_K^*} = \Gamma' \left(\frac{d\sigma_T}{d\Omega_K^*} + \epsilon \frac{d\sigma_L}{d\Omega_K^*} + \epsilon \frac{d\sigma_{LT}}{d\Omega_K^*} cos(2\phi_K^*) + \sqrt{\epsilon(\epsilon+1)} \frac{d\sigma_{TT}}{d\Omega_K^*} cos(\phi_K^*) \right)$$

With

$$\chi = \frac{1}{16 W m_P} \frac{|\boldsymbol{p}_K^*|}{K_H} \qquad K_H = \omega_{\text{lab}} - \frac{Q^2}{2m_P}$$

$$\epsilon = \frac{4EE' - Q^2}{2(E^2 + E'^2) + Q^2} \qquad \Gamma' = \frac{\alpha}{2\pi^2} \frac{\epsilon_2^{lab}}{\epsilon_1^{lab}} \frac{(\omega_{lab} - \frac{Q^2}{2m_N})}{Q^2} \frac{1}{1-\epsilon}$$

Study of sensitivity: Legendre moments

Expansion in terms of Legendre moments: a way to probe the sensitivity to a hybrid baryon contribution

$$P_m = \frac{2m+1}{2}\int_{-1}^{1} L_m(x) f(x) dx$$

$$L_m(x) = \sum_{j=0}^{m} a_{mj} x^j \qquad a_{mj} = (-1)^{(m-j)/2} \frac{1}{2^m} \frac{(m+j)!}{\left(\frac{(m-j)}{2}\right)! \left(\frac{(m+j)}{2}\right)! j!} \qquad m-j = even$$

$$L_0 = 1$$

$$L_1 = cos\vartheta$$

$$L_2 = \frac{1}{2}(3cos\vartheta^2 - 1)$$

$$L_3 = \frac{1}{2}(5cos\vartheta^3 - 3cos\vartheta)$$

$$L_4 = \frac{1}{8}(35cos\vartheta^4 - 30cos\vartheta^2 + 3)$$

$$L_5 = \frac{1}{8}(63cos\vartheta^5 - 70cos\vartheta^3 + 15cos\vartheta)$$

$$L_6 = \frac{1}{16}(231cos\vartheta^6 - 315cos\vartheta^4 + 105cos\vartheta - 5)$$

The appearance of a structure in a single Legendre moment at the same value of W for each Q^2 point is likely a signal from a resonance contribution.

Estimation of errors

Smearing with a gaussian

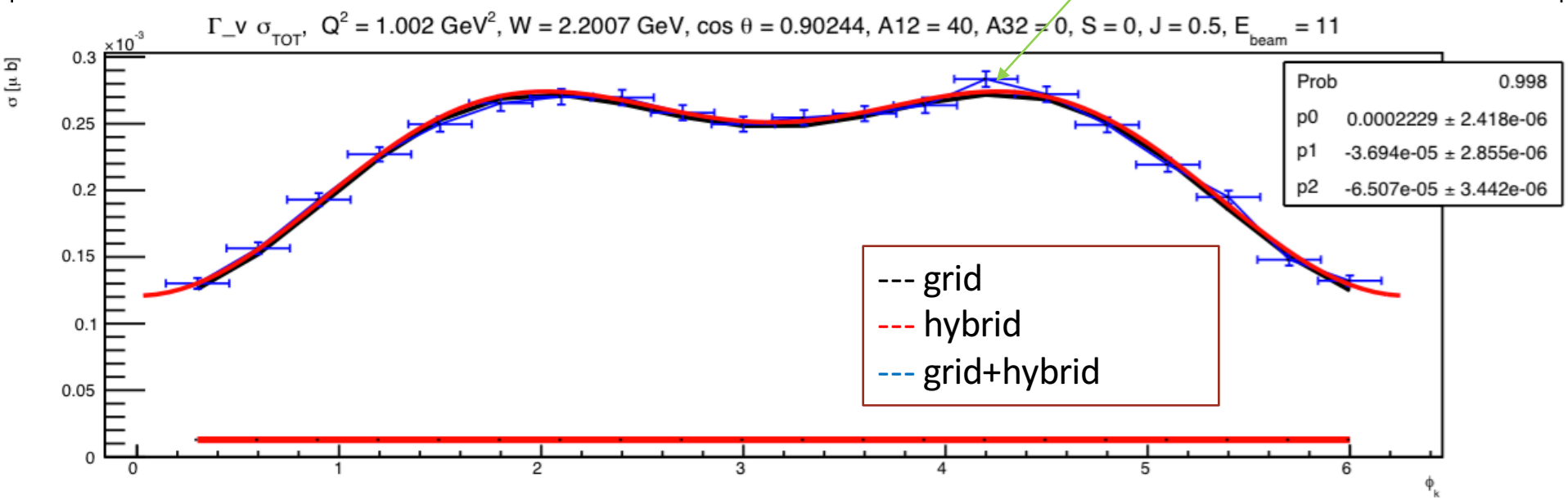

- J = 1/2
- Grid: Regge + Res.
- Q^2 = 1.002 GeV^2
- $A_{1/2}$ = 40 10^{-3} $GeV^{-1/2}$
- W = 2.2007 GeV
- cos ϑ= 0.90244

Extraction of cross sections with a fit:

$$\frac{d^4\sigma}{dW dQ^2 d\Omega_k} = \Gamma_v[\sigma_T + \varepsilon\sigma_L + \varepsilon\sigma_{TT} cos2\varphi_k + \sqrt{\varepsilon(\varepsilon+1)}\sigma_{LT} cos\varphi_k]$$

p_0 + err(p_0) p_1 + err(p_1) p_2 + err(p_2)

LT: Legendre moments analysis

Significant structures appear in most of the Legendre moments at the value of W = 2.2 GeV, corresponding to the mass of the added hybrid baryon

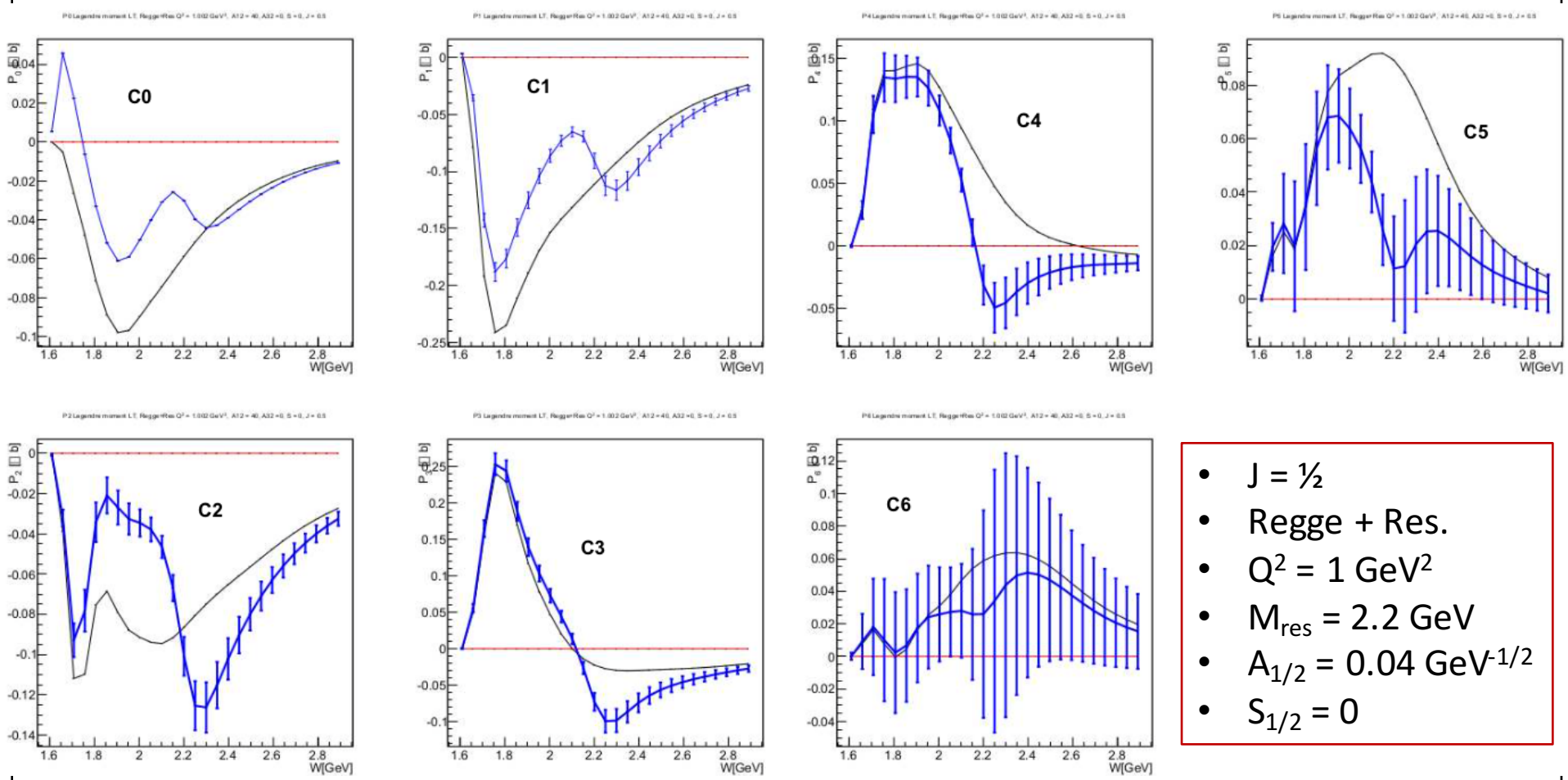

- J = ½
- Regge + Res.
- Q^2 = 1 GeV^2
- M_{res} = 2.2 GeV
- $A_{1/2}$ = 0.04 $GeV^{-1/2}$
- $S_{1/2}$ = 0

--- RPR --- hybrid --- RPR+hybrid

TT: Legendre moments analysis

Significant structures appear in most of the Legendre moments at the value of W = 2.2 GeV, corresponding to the mass of the added hybrid baryon

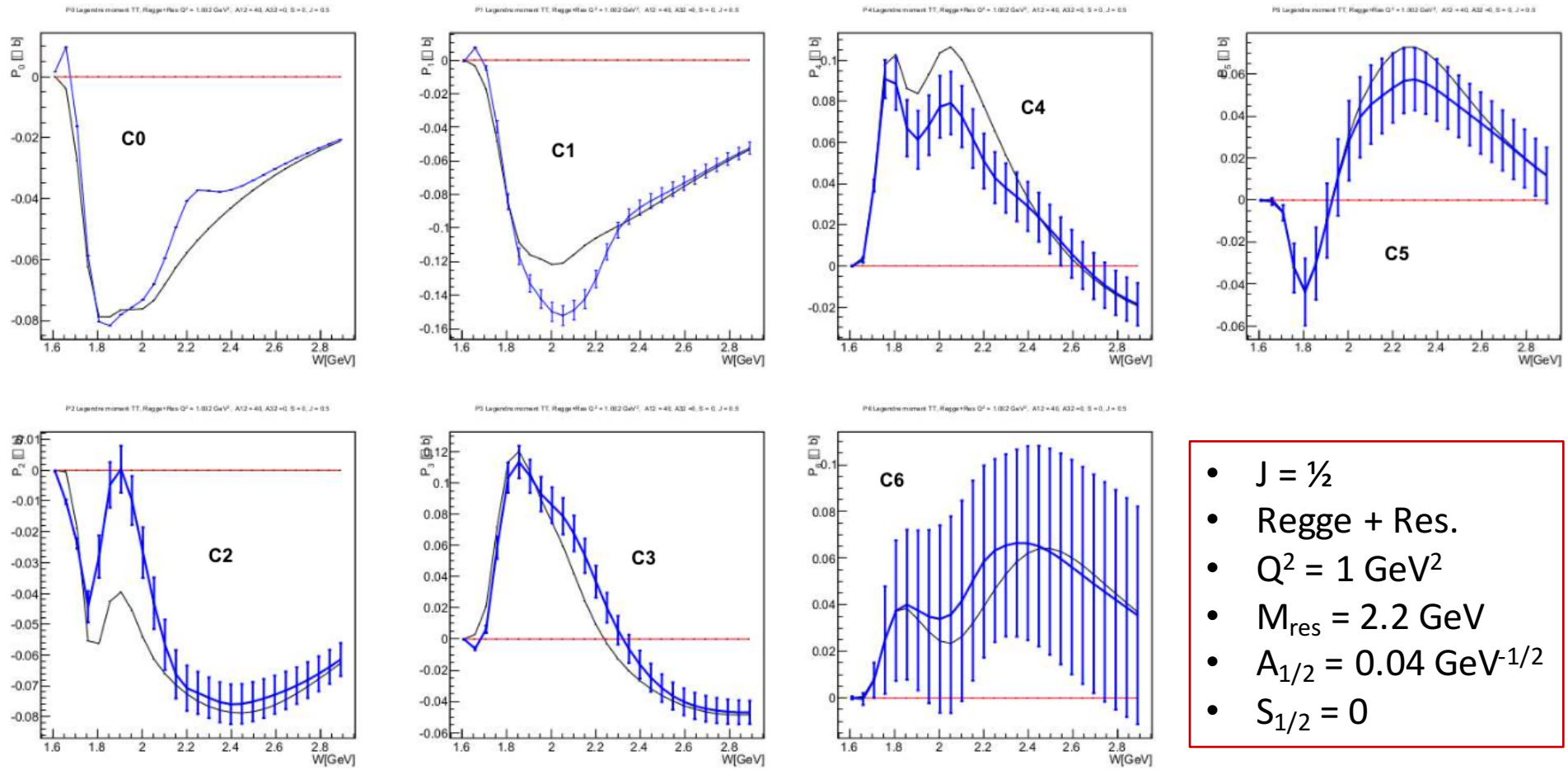

- J = ½
- Regge + Res.
- Q^2 = 1 GeV^2
- M_{res} = 2.2 GeV
- $A_{1/2}$ = 0.04 $GeV^{-1/2}$
- $S_{1/2}$ = 0

--- RPR --- hybrid --- RPR+hybrid

χ^2 vs $A_{1/2}$

The dependency of χ^2 calculated as

$$\chi^2 = \frac{1}{N_{d.p.}} \sum_W \frac{(P_m^{model\,+\,hybrid,\ variable\ A_{1/2}} - P_m^{model})^2}{\delta^2}$$

on a variable $A_{1/2}$ has been estimated for Legendre moments $P_0,\ldots,P_6$ for different configurations:

- E_{beam} = 6.6 GeV, 8.8 GeV
- Q^2 = 0.1 GeV^2, 0.562 GeV^2, 1.002 GeV^2

For each curve the value of $A_{1/2}$ for which the χ^2 exceeds 4 has been obtained.

U Legendre moment: χ^2 vs $A_{1/2}$

σ_U χ^2/d.p. vs A1/2 , Q^2 = 0.1 GeV^2 E = 6.6 GeV

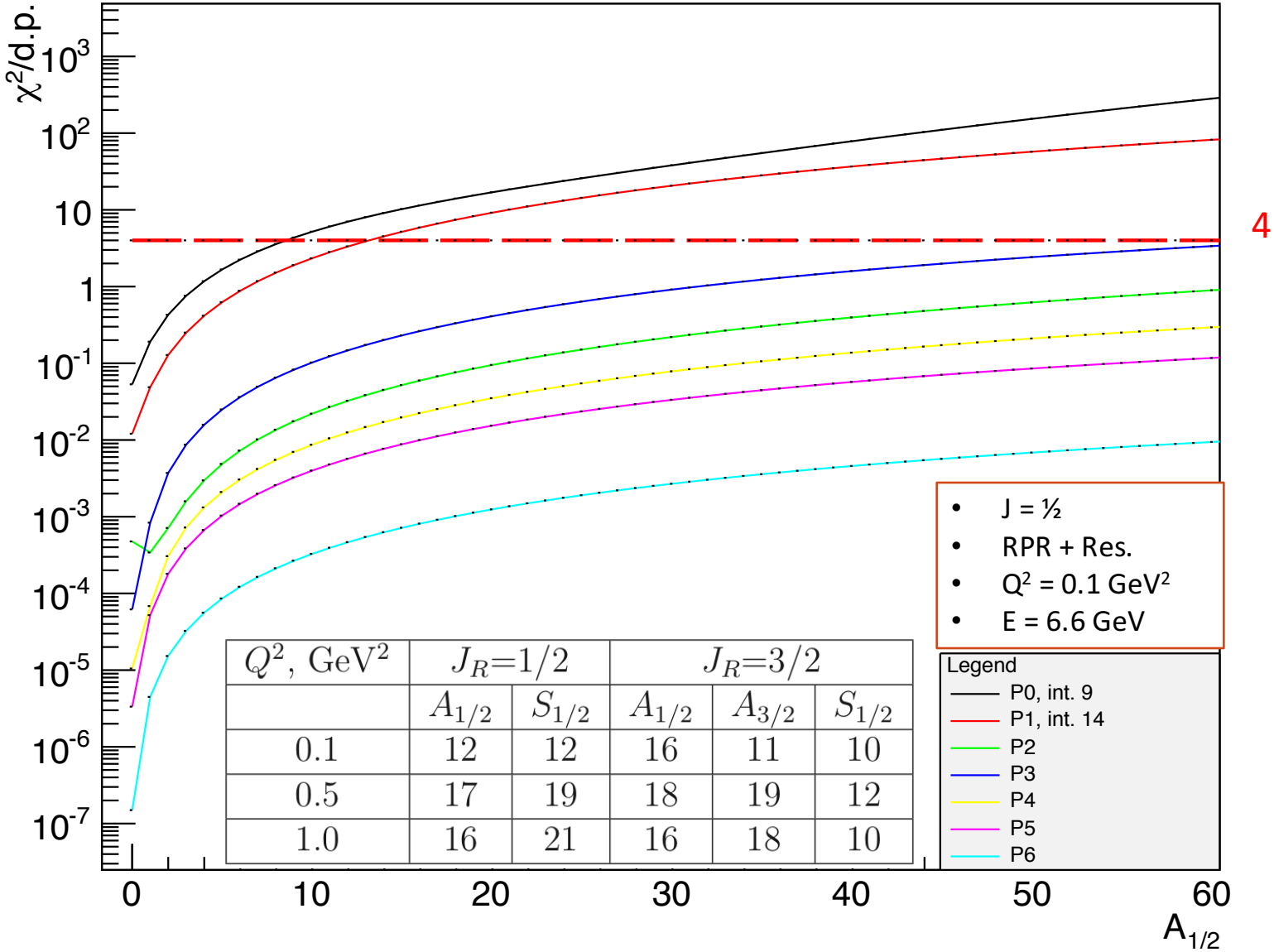

Q^2, GeV^2	J_R=1/2		J_R=3/2		
	$A_{1/2}$	$S_{1/2}$	$A_{1/2}$	$A_{3/2}$	$S_{1/2}$
0.1	12	12	16	11	10
0.5	17	19	18	19	12
1.0	16	21	16	18	10

χ^2 vs M_{res}

The dependency of χ^2 calculated as

$$\chi^2 = \frac{1}{N_{d.p.}} \sum_W \frac{(P_m^{model\,+\,hybrid\,with\,M_{res}=2.2\,GeV} - P_m^{model\,+\,hybrid\,with\,variable\,M_{res}})^2}{\delta^2}$$

on a variable M_{res} has been estimated for Legendre moments $P_0,\ldots,P_6$ for different configurations:

- E_{beam} = 6.6 GeV, 8.8 GeV
- $A_{1/2}$ = 20, 40 [10^{-3} $GeV^{-1/2}$]
- Q^2 = 0.1 GeV^2, 0.562 GeV^2, 1.002 GeV^2

U Legendre moment: χ^2 vs M_{res}

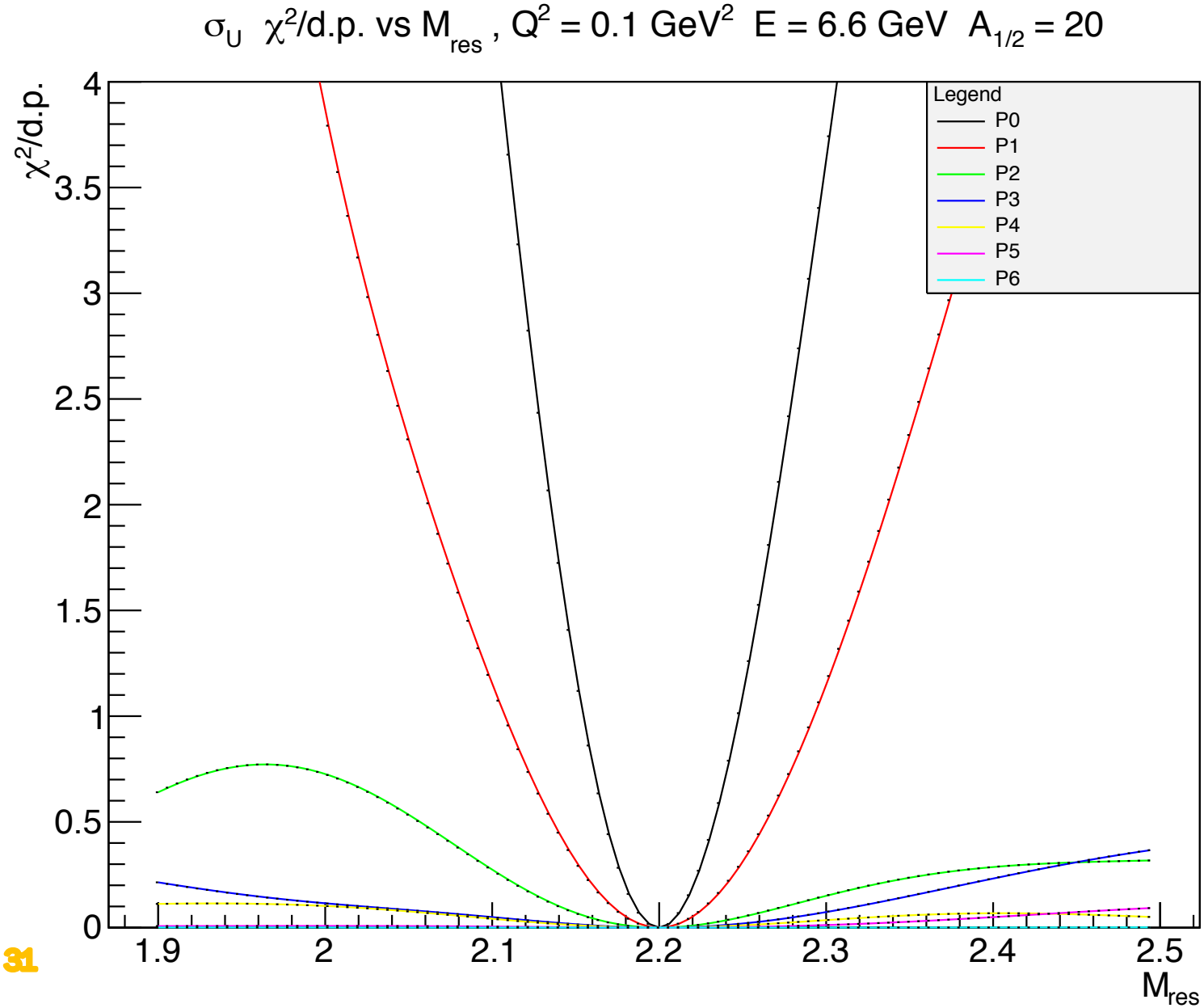

- J = ½
- RPR with res.
- Q^2 = 0.1 GeV^2
- E = 6.6 GeV
- A = 0.02 GeV$^{-1/2}$

χ^2 vs M_{res} and A

The χ^2 has been calculated as:

$$\chi^2 = \frac{1}{N_{d.p.}} \sum_{W,cos\vartheta\ \varphi} \frac{(\sigma_{fixed} - \sigma_{variable})^2}{\delta^2} = \frac{1}{N_{d.p.}} \sum_{W,cos\vartheta\ \varphi} \left(\frac{\sigma_{fixed} - \sigma_{variable}}{\sigma_{variable}}\right)^2 N_{ev}$$

Where

- σ_{fixed}: model + hybrid, 2 resonances
  - Resonance 1: $J = \frac{1}{2}, A_{1/2} = fixed, M^1_{res} = 2.1\ GeV$
  - Resonance 2: $J = \frac{3}{2}, A_{3/2} = fixed, A_{1/2} = fixed, M^3_{res} = 2.2\ GeV$
- $\sigma_{variable}$: model + hybrid, 2 resonances
  - Resonance 1: $J = \frac{1}{2},\ A_{1/2} = variable(0 - 50, step\ 1), M^1_{res} = variable(1.8 - 2.5\ GeV, step\ 20\ MeV)$
  - Resonance 2: $J = \frac{3}{2}, A_{\frac{3}{2}} = variable\ (0 - 50, step\ 1), A_{1/2} = variable(0 - 50, step\ 1), M^3_{res} = variable\ (1.8 - 2.5\ GeV, step\ 20\ MeV)$
- N_{ev} = number of expected events in 50 days beamtime for each bin in Q^2 , $W, cos\vartheta, \varphi$

χ^2 has been estimated for variable M^1_{res} , M^3_{res} and $A_{1/2} = A_{3/2}$ for the configurations:

- $(J^+_{1/2} : A_{1/2}, J^+_{3/2} : A_{1/2}, A_{3/2}) = (10, 10, 10), (20, 20, 20), (40, 40, 40)$
- $E_{beam} = 6.6$ GeV
- $Q^2 = 0.562\ GeV^2$
- $\Gamma_{res} = 0.25$ GeV

A_{fixed}=20: χ^2 vs M_{res} and A

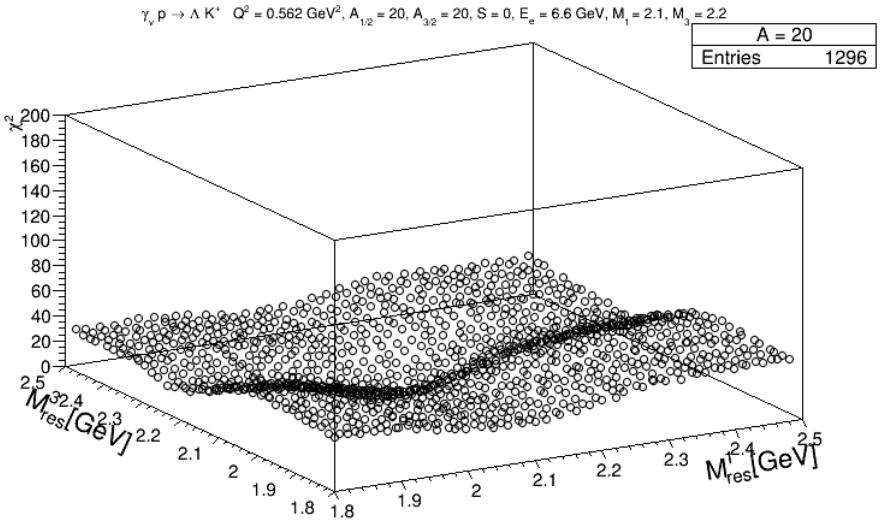

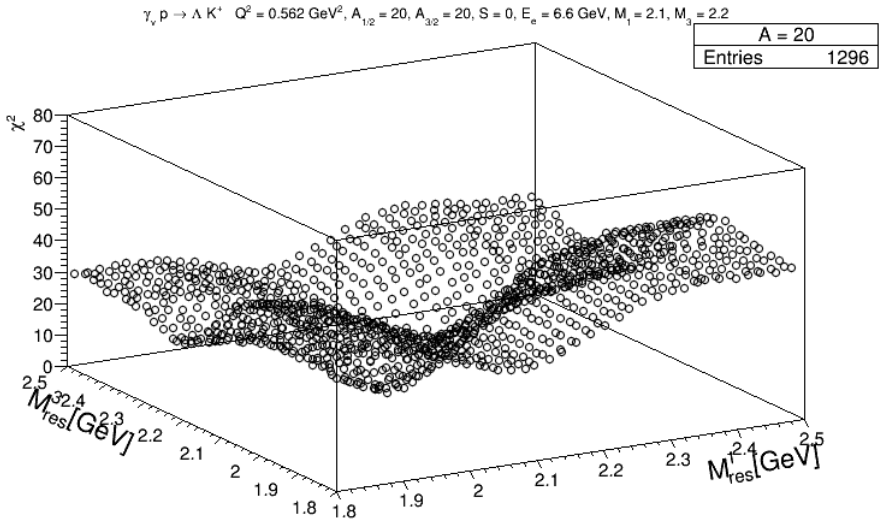

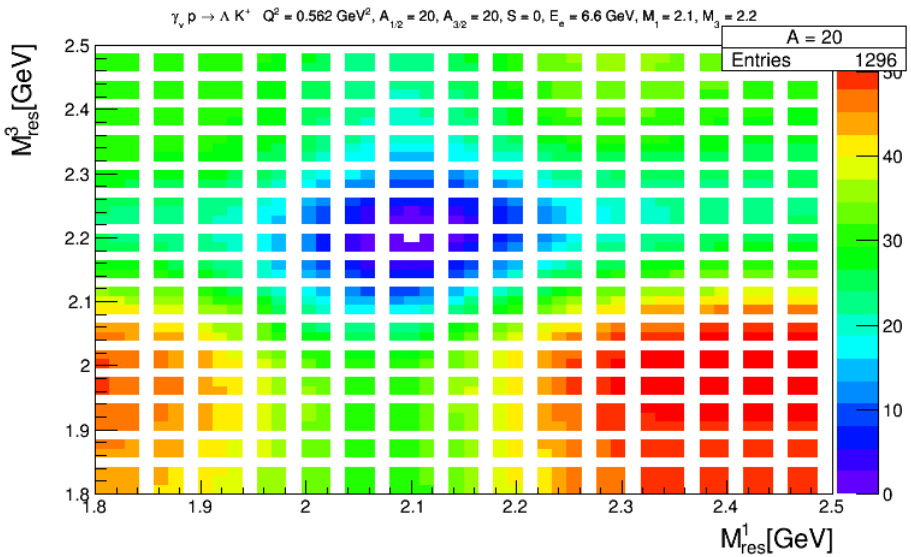

A_{fixed}=20: χ^2 vs M_{res} and A

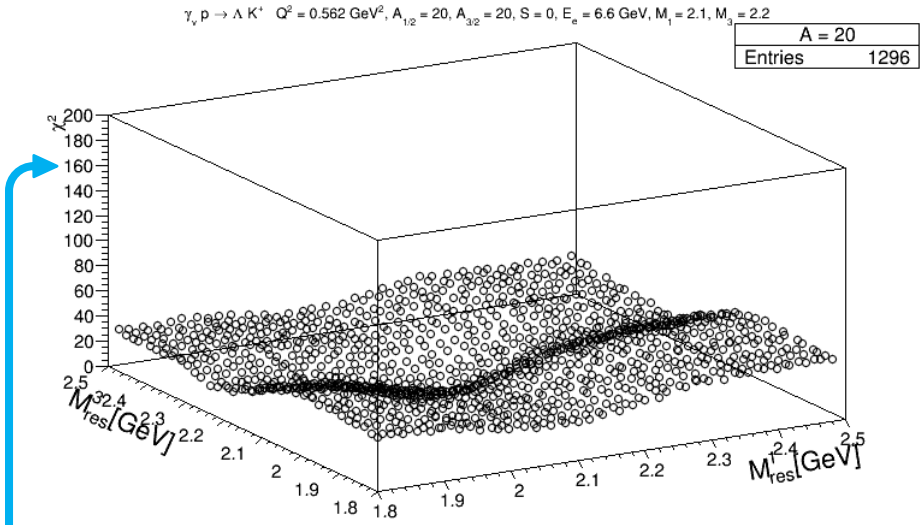

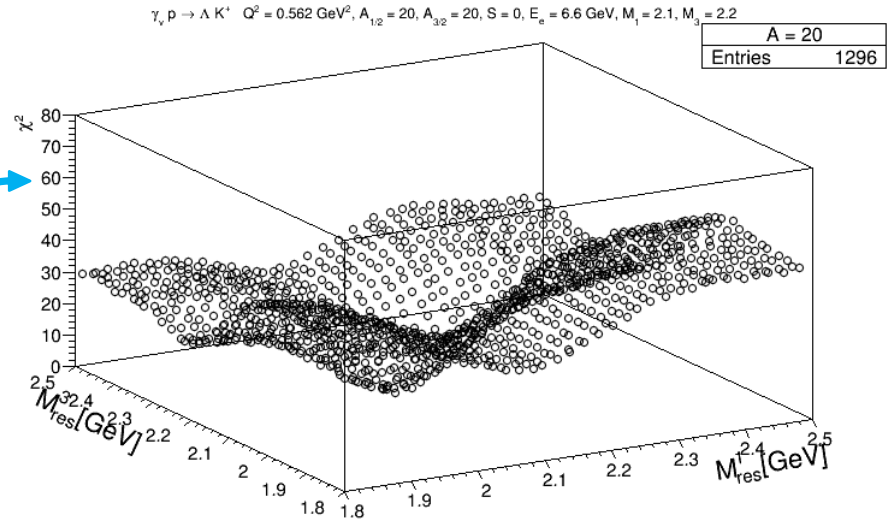

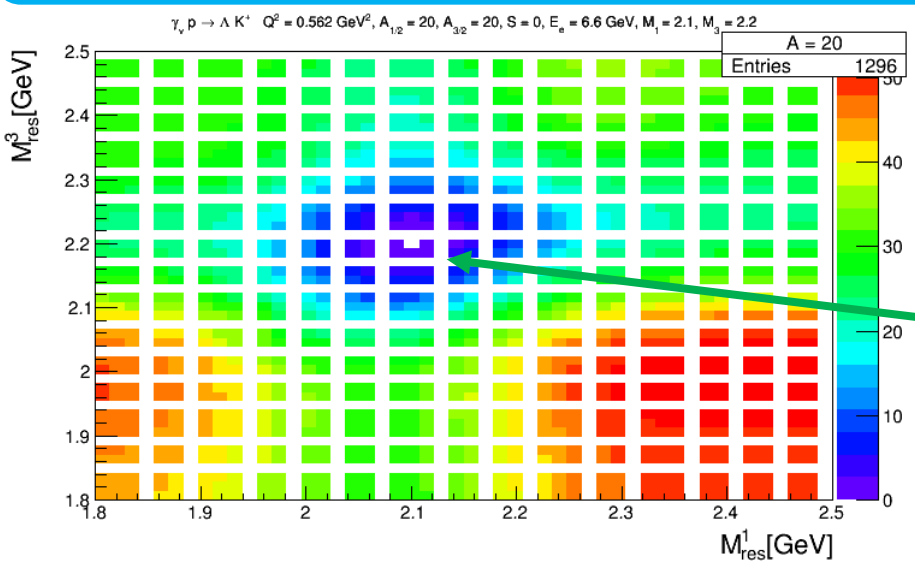

Two different scales

Minimum

Conclusions

Simulation and fast mc reconstruction of $K^{+}\Lambda$ electro-production events in CLAS12

- Run condition: E_{beam}=6.6 GeV and Torus Current = -3375 A presents good values of efficiency
- Search of hybrid baryons in runs with standard conditions of magnet and beam energy can be integrated with dedicated runs.

Study of sensitivity

- Hybrid resonance has been added at **amplitude level** to study the sensitivity of our system to a hybrid resonance
- Legendre moments analysis has been employed as a way to identify resonances
- Simulations demonstrated:
  - Possibility to observe hybrid baryon signal with electrocoupling values above 0.01 $GeV^{-1/2}$
  - Credible reconstruction of the hybrid resonance parameters from the data

Future Work

Next step:

- Full implementation in CLAS12 simulation and reconstruction
  - GEMC
  - CLARA framework

- Reconstruction of the interaction strength from simulated data

Future Work

Next step:

- Full implementation in CLAS12 simulation and reconstruction
  - GEMC
  - CLARA framework

- Reconstruction of the interaction strength from simulated data

Thank you

Bibliography

- *CLAS12 Forward Tagger (FT) Technical Design Report*, The CLAS12 Collaboration
- *Draft CLAS-Note, An Inner Calorimeter for CLAS/DVCS experiments*, I. Bedlinskiy, et Al.
- *CLAS/DVCS Inner Calorimeter Calibration*, R. Niyazov , S. Stepanyan
- *A Letter of Intent to the Jefferson Lab PAC43, Search for Hybrid Baryons with CLAS12 in Hall B*, A. D'Angelo et al.
- J. Dudek et al., 2012
- V. Mokeev et al., 2012, *Experimental study of the P11(1440) and D13(1520) resonances from the CLAS data on* $ep \rightarrow e\pi^+\pi^- p$
- I. G. Aznauryan et al., CLAS Collaboration, PHYSICAL REVIEW C 80, 055203 (2009)
- [1] S. Capstick and B. D. Keister, Phys. Rev. D 51, 3598 (1995)
- [2] I. G. Aznauryan, Phys. Rev. C 76, 025212 (2007).
- [3] Z. P. Li, V. Burkert, and Zh. Li, Phys. Rev. D 46, 70 (1992).

Separating Q^3G from Q^3 states: $A_{1/2}(Q^2)$ and $S_{1/2}(Q^2)$

The ***N**** **hadronic decay amplitudes** can be expanded in **partial waves** of total momentum *J*

$\nu = -\lambda_\Delta$

CM polar and azimuthal angles for the final K

$$\langle \lambda_f | T_{dec} | \lambda_R \rangle = \langle \lambda_f | T^{J_r}_{dec} | \lambda_R \rangle d^{J_r}_{\mu\nu}(\cos\theta^*) e^{i\mu\phi^*}$$

λ_R

where

N^* spin

partial hadronic decay widths of the N^* to $k\Lambda$ final states f of helicity λ_f

Magnitudes of the three-momenta of the final K for the $N^* \rightarrow K\Lambda$ decay, evaluated at $W = M_r$ and at the running W, respectively, and averaged over the running mass of the unstable hadron in the intermediate state

$$\langle \lambda_f | T^{J_r}_{dec} | \lambda_R \rangle = \frac{2\sqrt{2\pi}\sqrt{2J_r+1}\,M_r\sqrt{\Gamma_{\lambda_f}}}{\sqrt{\langle p_i^r \rangle}} \sqrt{\frac{\langle p_K^r \rangle}{\langle p_K \rangle}}$$

The **resonance electroexcitation amplitudes** can be related to the $\gamma_v NN^*$ electrocouplings $\mathbf{A_{1/2}}$, $\mathbf{A_{3/2}}$, and $\mathbf{S_{1/2}}$ for nucleons

$$\langle \lambda_R | T_{em} | \lambda_\gamma \lambda_p \rangle = \frac{W}{M_r}\sqrt{\frac{8 M_N M_r q_{\gamma_r}}{4\pi\alpha}}\sqrt{\frac{q_{\gamma_r}}{q_\gamma}} A_{1/2,3/2}(Q^2) \quad \text{with} \quad |\lambda_\gamma - \lambda_p| = \frac{1}{2}, \frac{3}{2} \text{ for transverse photons,}$$

$$\langle \lambda_R | T_{em} | \lambda_\gamma \lambda_p \rangle = \frac{W}{M_r}\sqrt{\frac{16 M_N M_r q_{\gamma_r}}{4\pi\alpha}}\sqrt{\frac{q_{\gamma_r}}{q_\gamma}} S_{1/2}(Q^2) \text{ for longitudinal photons}$$

$q_{\gamma,r}$ is the three-momentum modulus of the photon at $W = M_r$ in the CM frame

$$q_\gamma = \sqrt{Q^2 + E_\gamma^2}$$

CLAS Collaboration, PHYSICAL REVIEW C 86, 035203 (2012)

Separating Q^3G from Q^3 states

Transverse elicity amplitude $A_{1/2}(Q^2)$ and longitudinal elicity amplitude $S_{1/2}(Q^2)$ allow to distinguish Q^3G from Q^3 states

Z.P. Li, V.B., Zh. Li, Phys.Rev. D46 (1992) 70

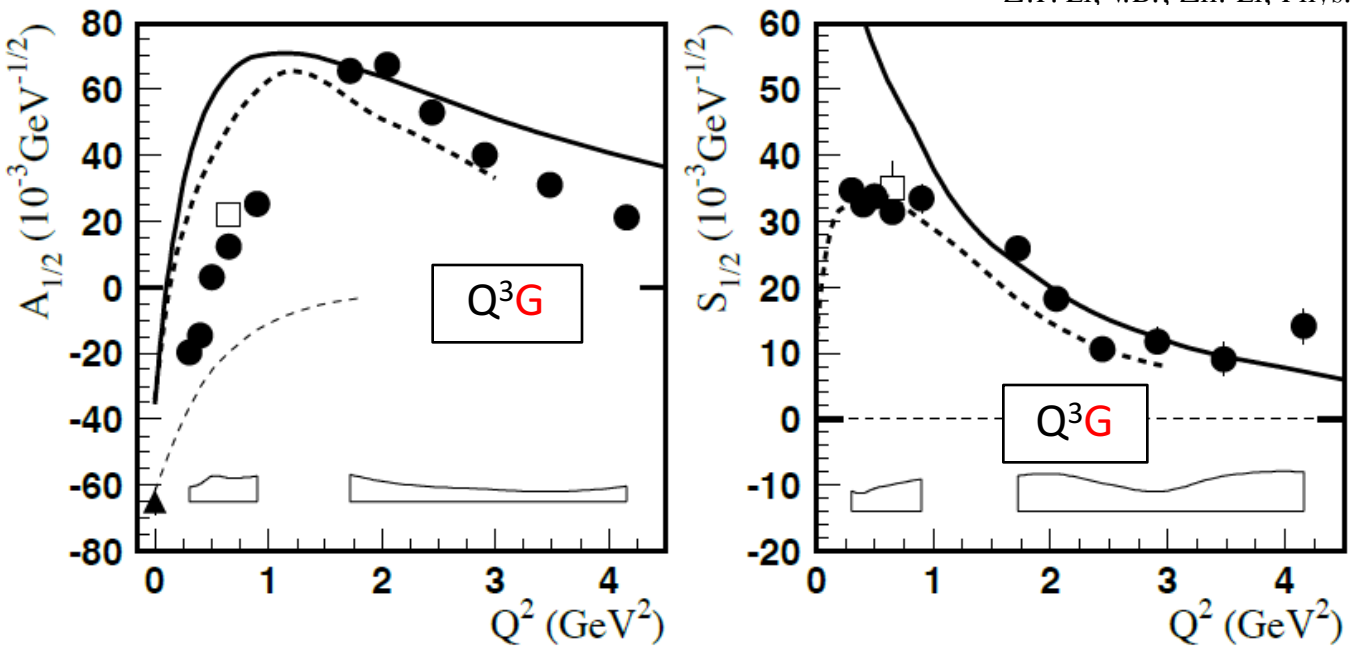

Helicity amplitudes for the $\gamma^* p \rightarrow N(1440)P11$ transition. The full circles are the results obtained from CLAS data. The bands show the model uncertainties. The open boxes are the results of the combined analysis of CLAS single π and 2π electroproduction data. The full triangle at Q2 = 0 is the RPP estimate. The thick curves correspond to the results obtained in the LF relativistic quark models assuming that N(1440)P11 is a first radial excitation of the 3q ground state: (dashed), (solid). The thin dashed curves are obtained assuming that N(1440)P11 is a gluonic baryon excitation (q3G hybrid state)

Trigger conditions and simulations

Step 1

Selection of trigger conditions for fastmc event generator:

- 1 electron in CLAS
- 1 charged particle in CLAS

Or

- 1 electron in FT
- 2 charged particles in CLAS

- 1 electron

- 1 electron + 2 charged particle

Charged particle: proton, π^-, k^+

Step 2

Production of plots with the conditions:

- E_{beam} = 6.6 GeV, 8.8 GeV, 11 GeV

- Torus current = ±1500 A, ±2950 A, ±3370 A

The Tracker (FT-Trck)

Micromegas detectors exploit the gas ionization process with charged particles to:

- Reconstruct the electron point of impact and path

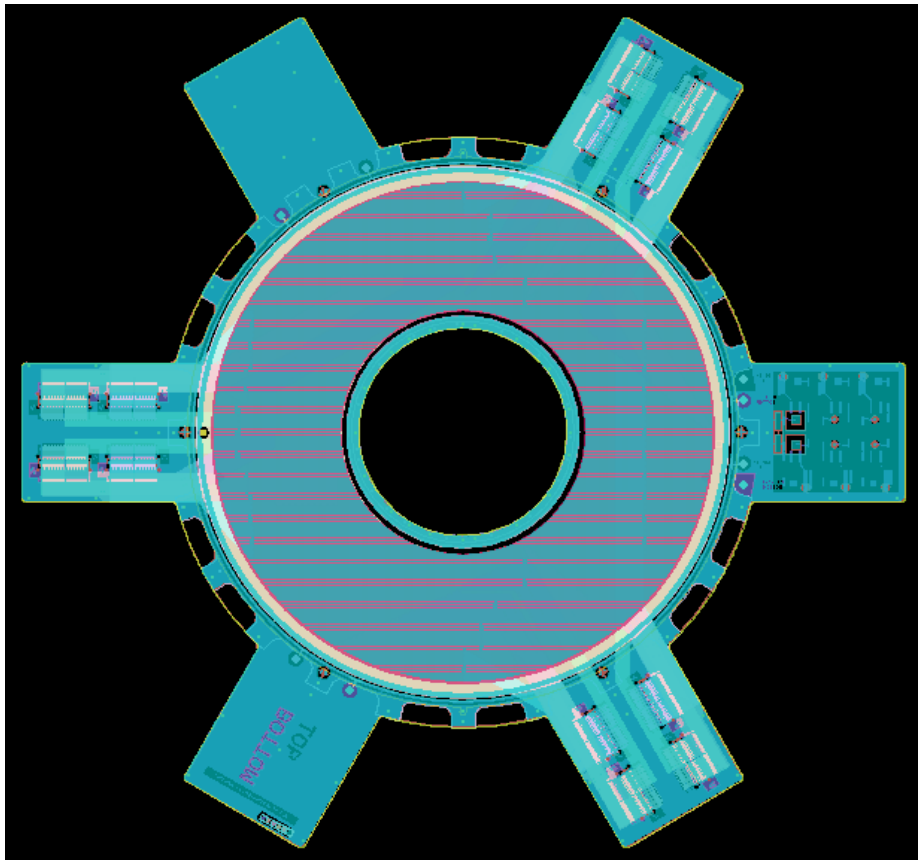

Two layers of pairs of Micromegas detectors with strip readout

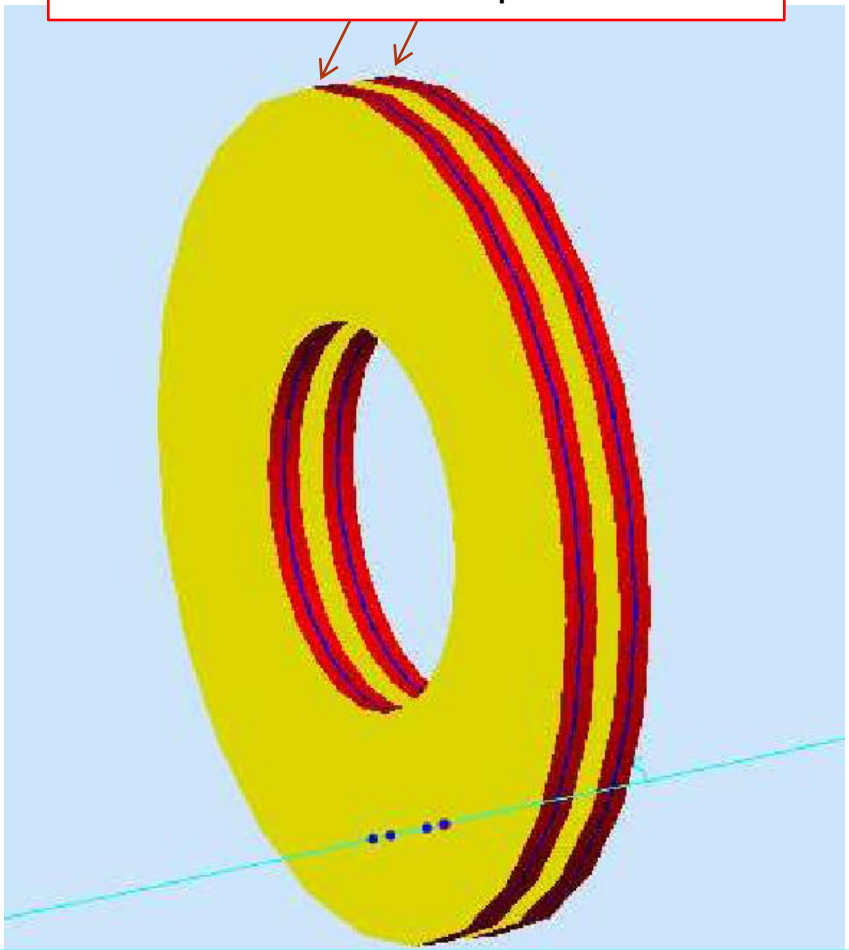

The strips of two different Micromegas in the same layer are orthogonal to produce a (x,y) couple

The Hodoscope (FT-Hodo)

E released in the hodoscope by an e^-

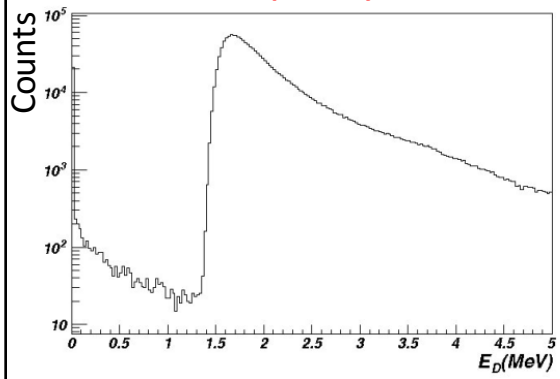

E released in the hodoscope by a γ

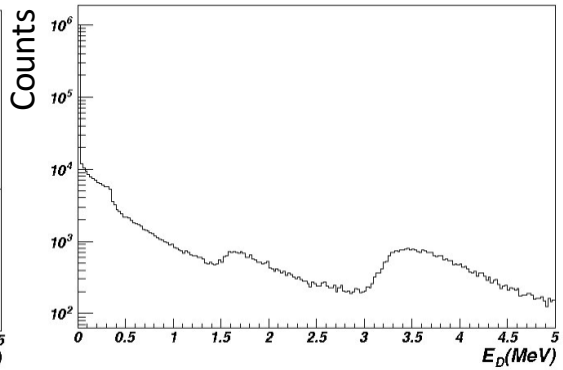

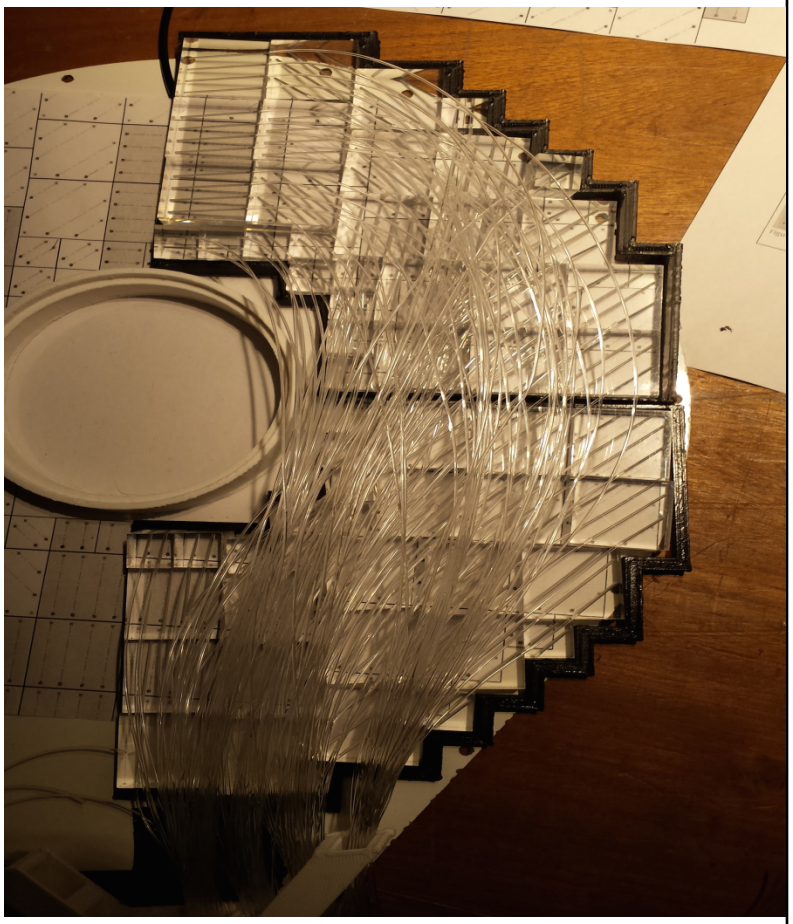

232 scintillator tiles, 752 fibers in total

Wavelength shifting (WLS) fibres

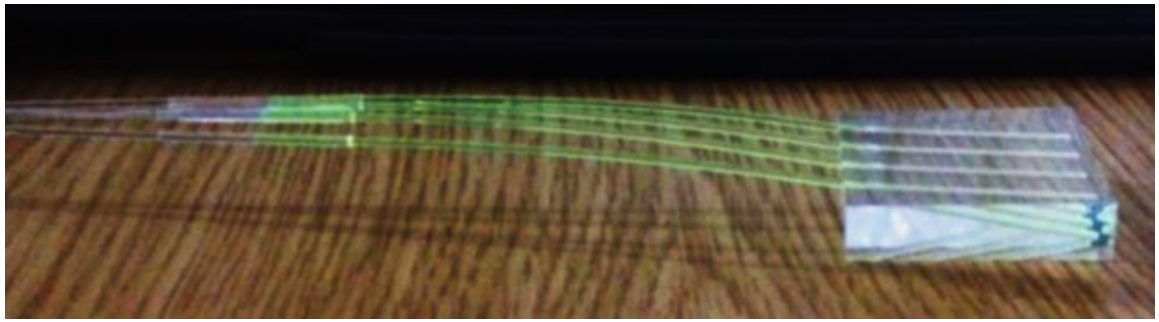

Two layers of plastic **scintillator tiles**

The Electromagnetic Calorimeter (FT-Cal)

Requirements:

- High radiation hardness
- High light yield
- Small radiation length and Moliere radius
- Fast recovery time
- Good energy and time resolution

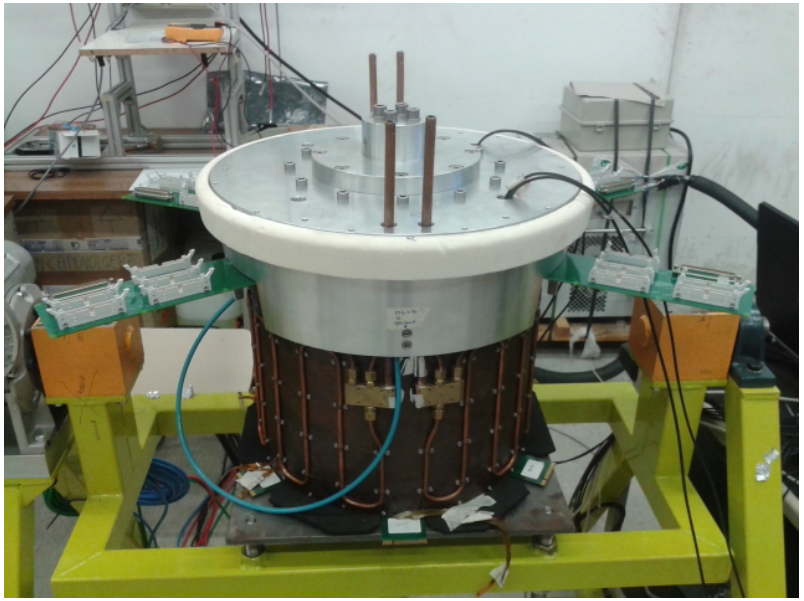

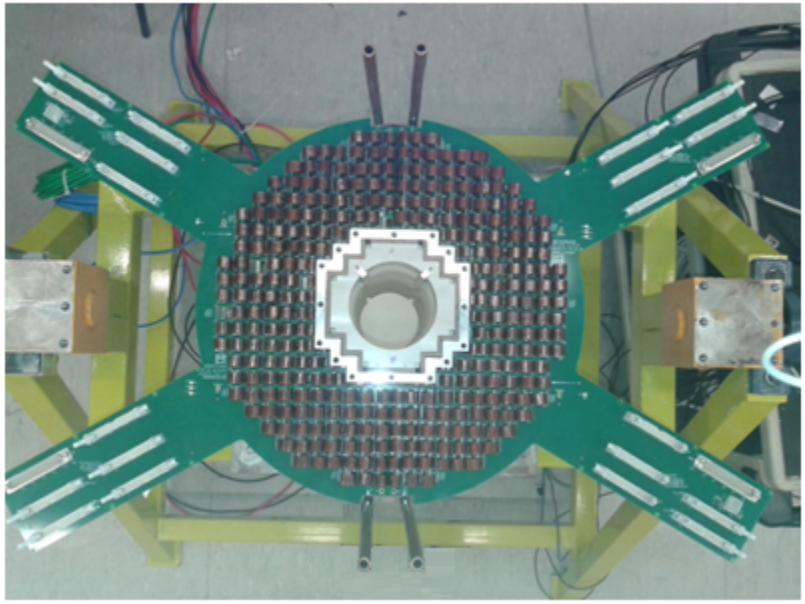

Modules of $PbWO_4$ scintillating crystals

Pros	Contra
•High density (8.28 g/cm^3) •Small radiation lenght (0.9 cm) •Very fast decay time (6.5 ns) •Very high radiation hardness	•Poor LY (fraction of % of the NaI one) (100-200 γ/MeV) •Temperature must be controlled to avoid variations in gain and noise